Planetary boundary layer and atmospheric turbulence.

Szymon P. Malinowski
Marta Wacławczyk

Institute of Geophysics UW

2017/18

Lecture 10

Simplified set of equations of cloud dynamics and thermodynamics:

$$D/Dt \equiv \partial/\partial t + \mathbf{v} \cdot \nabla$$

$$B \equiv g\left[\frac{T - T_0}{T_0} + \varepsilon(q_v - q_{v_0}) - q_c\right], \qquad (2)$$

$$\frac{D\mathbf{v}}{Dt} = -\nabla\pi + \mathbf{k}B + \nu\nabla^2\mathbf{v}, \qquad (1a)$$

$$\nabla \cdot \mathbf{v} = 0, \qquad (1b)$$

$$\frac{DT}{Dt} = \frac{L}{c_p}C_d + \mu_T\nabla^2 T, \qquad (1c)$$

$$\frac{Dq_v}{Dt} = -C_d + \mu_v\nabla^2 q_v, \qquad (1d)$$

$$\frac{Dq_c}{Dt} = C_d. \qquad (3)$$

Andrejczuk et al., 2004

NOTES AND CORRESPONDENCE

The Effects of Turbulent Mixing in Clouds

M. B. BAKER AND R. E. BREIDENTHAL

University of Washington, Seattle, 98195

T. W. CHOULARTON AND J. LATHAM

Physics Department, UMIST, Manchester, England

14 April 1983 and 2 September 1983

ABSTRACT

Turbulent mixing of cloudy and cloud-free air may play an important role in determining the overall dynamical and microphysical behavior of warm clouds. We present a model of turbulent mixing based on laboratory and theoretical studies of chemically reacting shear layers, extended to include the effects of buoyancy instabilities and droplet sedimentation. It is found to be consistent with recent observations of microphysical variability in natural clouds.

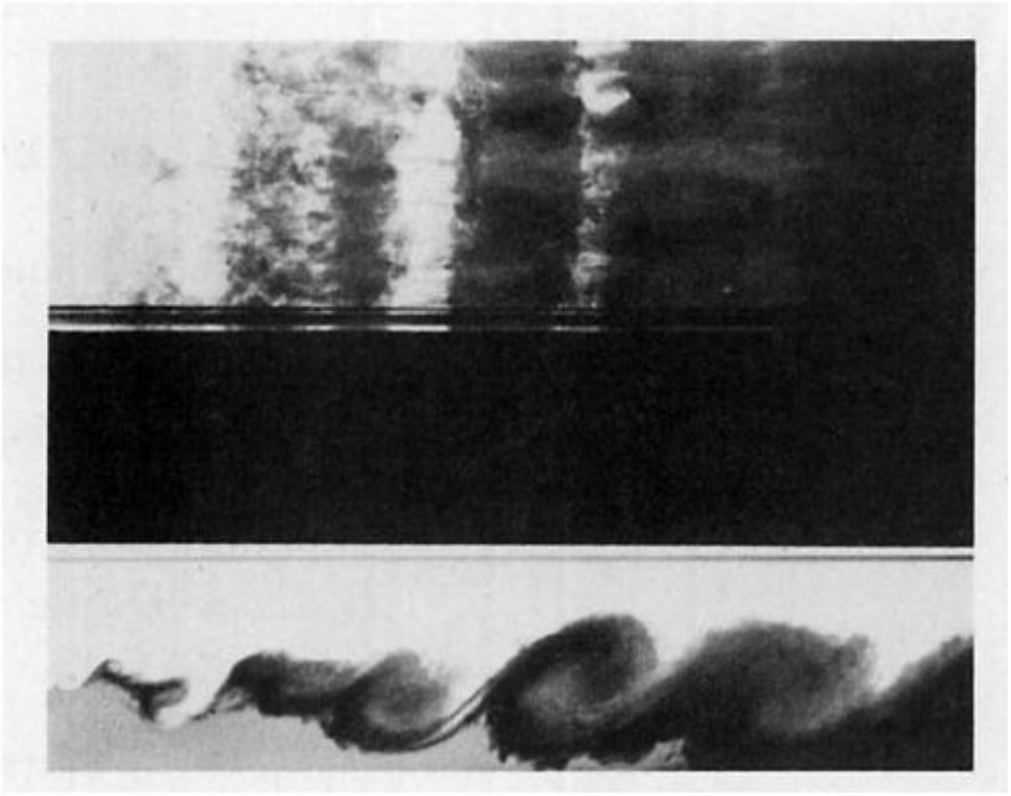

FIG. 1. Simultaneous plan (top) and side (bottom) views of a chemically reacting, plane shear layer. $\Delta UL/\nu \sim 10^4$.

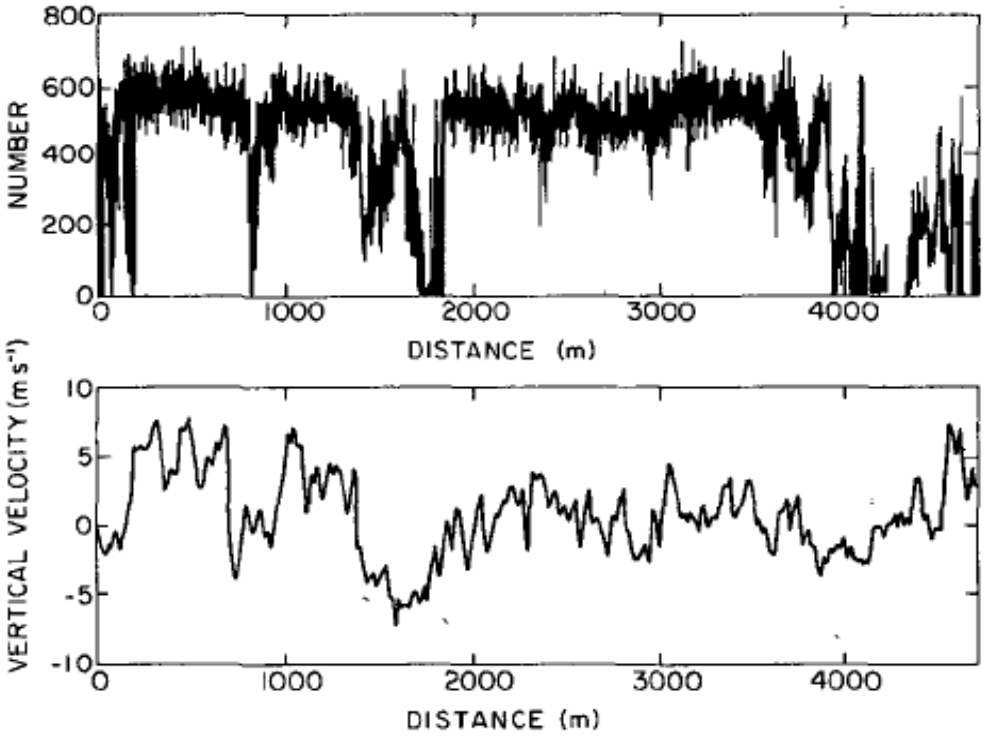

FIG. 2. Simultaneous measurements of droplet number and vertical velocity in a penetration of Montana cumulus (data courtesy of Dr. W. A. Cooper).

5. Conclusions

A simple model of turbulent mixing in the presence of buoyancy instabilities and sedimentation has been proposed to explain observed dynamic and microphysical variability in warm clouds. Rough estimates of droplet spectral variability caused by mixing indicate that sedimentation and buoyancy effects may be as important as shear-induced effects under a range of realistic conditions.

Cloud–Environment Interface Instability. Part II: Extension to Three Spatial Dimensions

WOJCIECH W. GRABOWSKI* AND TERRY L. CLARK

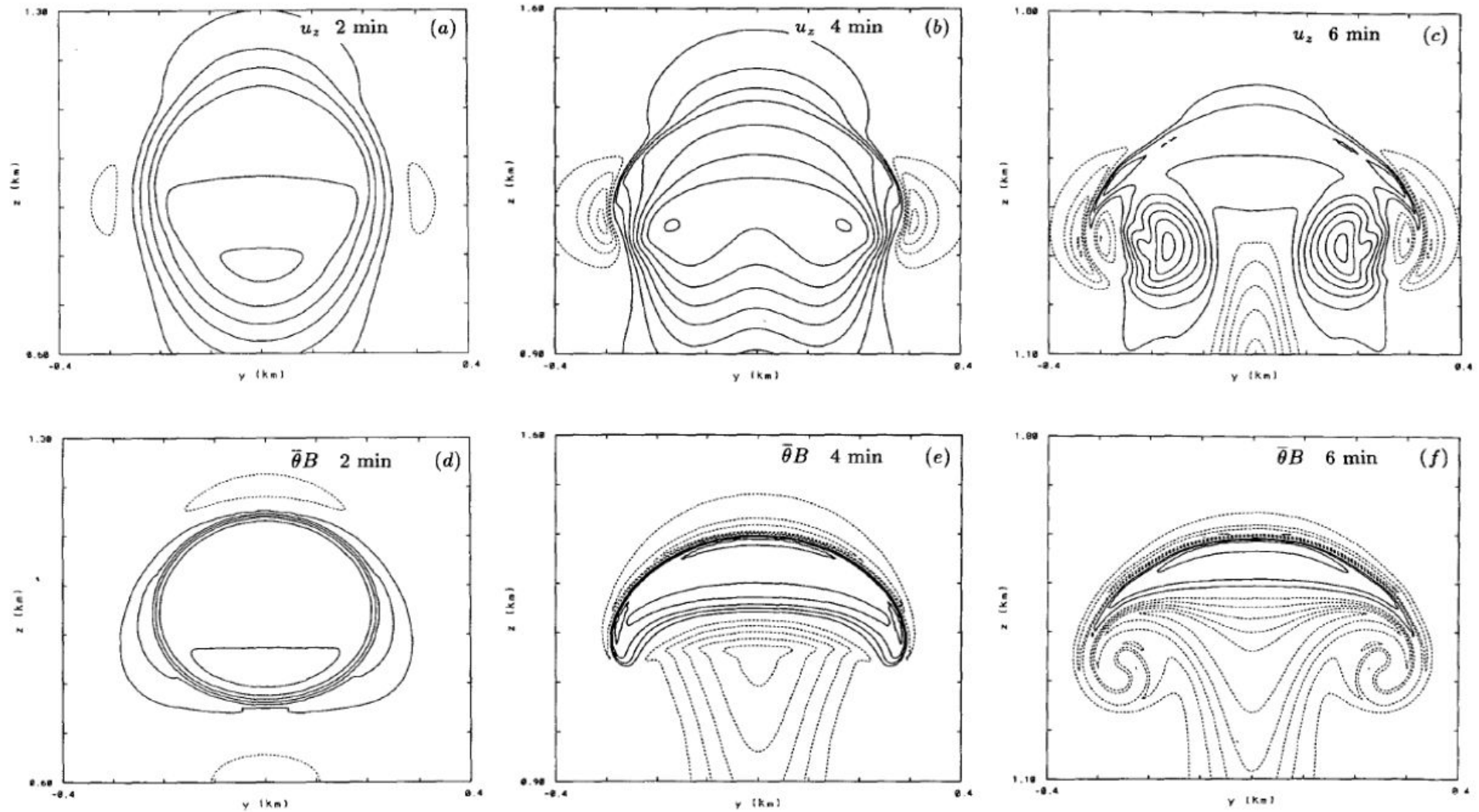

FIG. 1. Fields of vertical velocity (a, b, c), buoyancy (d, e, f), cloud water mixing ratio (g, h, i), and azimuthal component of vorticity (j, k, l) for t = 2, 4, and 6 min in the plane of symmetry x = 0. Contour interval is 0.5 m s^{-1} for u_z, 0.2 (d), 0.3 (e), and

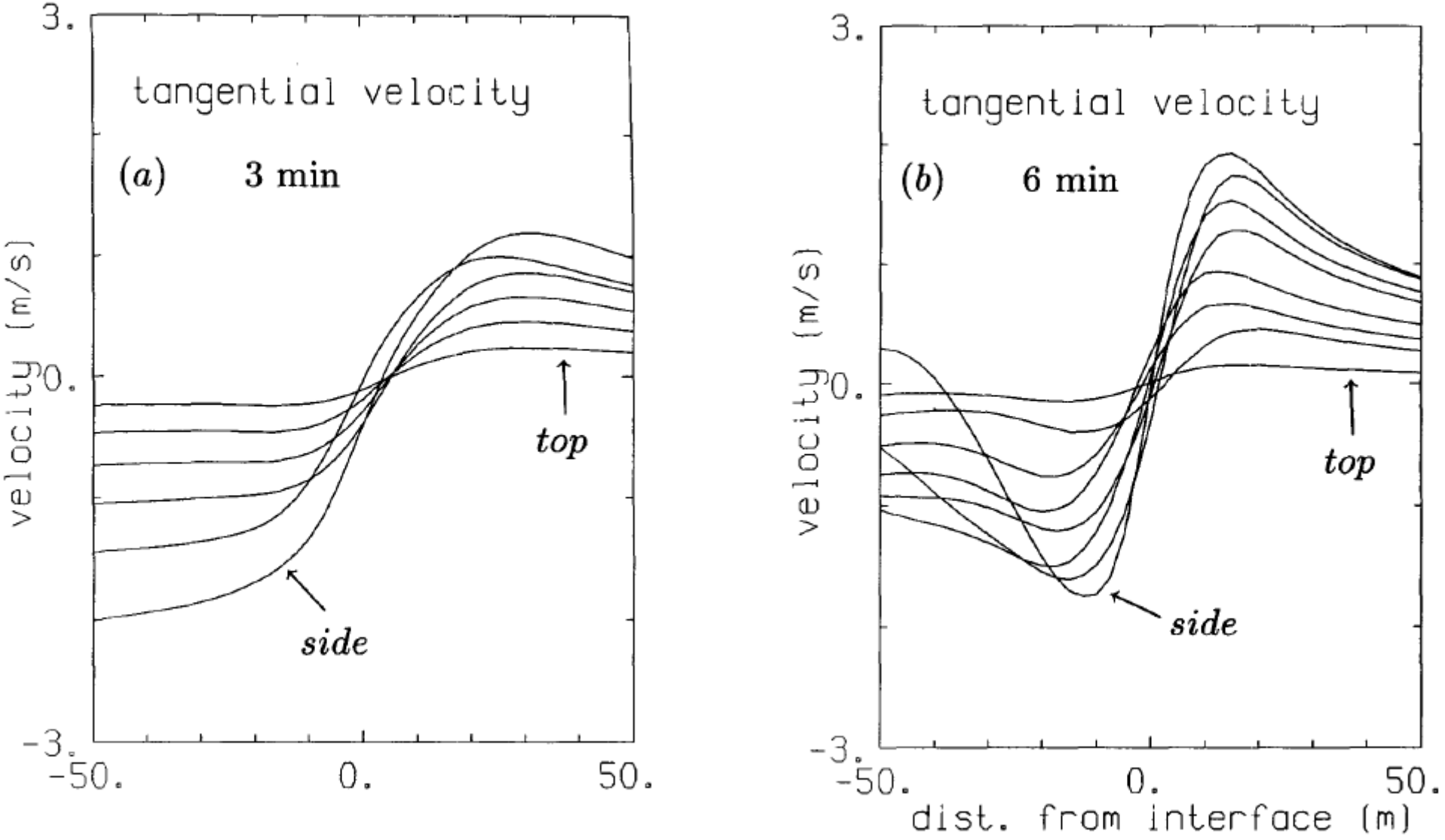

FIG. 2. Profiles of the tangential velocity u_t as a function of distance from the interface at $t = 3$ min (a) and 6 min (b) for several positions along the interface. Profiles at locations close to thermal top and close to the side are marked accordingly. Data are from experiment 3D6M.

JAS 2008

Subsiding Shells around Shallow Cumulus Clouds

THIJS HEUS AND HARM J. J. JONKER

Department of Multi-Scale Physics, Delft University of Technology, Delft, Netherlands

(Manuscript received 18 October 2006, in final form 5 June 2007)

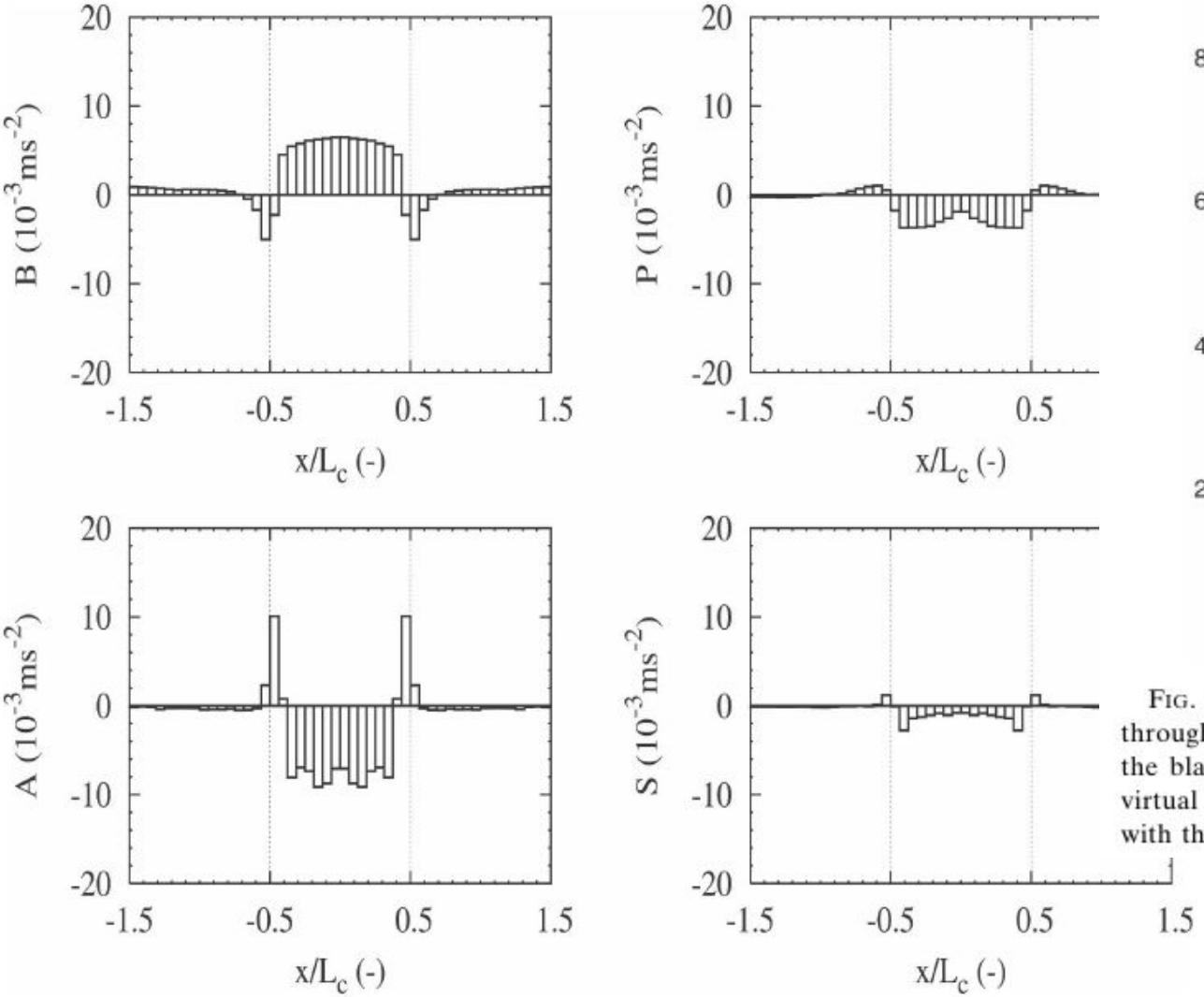

FIG. 2. The individual terms of the vertical momentum Eq. (1): (top left) buoyancy B, (top right) vertical pressure gradient P, (bottom left) advection A, and (bottom right) subgrid diffusion S, plotted against the distance to cloud center x (normalized with cloud size L_c).

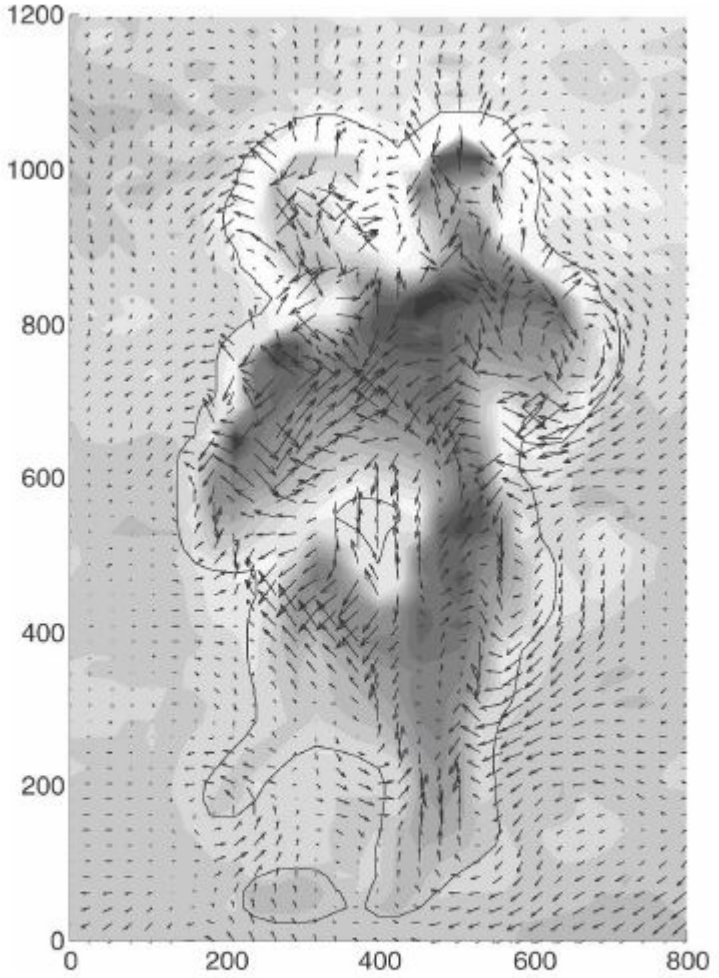

FIG. 5. A y–z plane cross section (with distances in meters) through the center of mass of a cloud. Cloud edge is denoted by the black line, the vectors signify the in-plane velocity, and the virtual potential temperature excess is displayed in gray tones, with the lighter areas more negatively buoyant.

FACT 1:
Combined measurements aimed at investigations of interaction between turbulence, thermodynamics (phase change) and microphysics (cloud droplets) in small scales have never been documented.
First reliable data from the in-situ measurements of small-scale turbulence in clouds become available just recently, and it will take time to cover a wide range of possible in-cloud conditions.

FACT 2:
In many theoretical studies turbulent velocities in small scales in clouds are assumed to be stationary, homogeneous and isotropic.
Clouds, however, are (almost always) nonstationary, inhomogeneous and anisotropic.
The last one holds even in small scales (gravity/buoyancy).

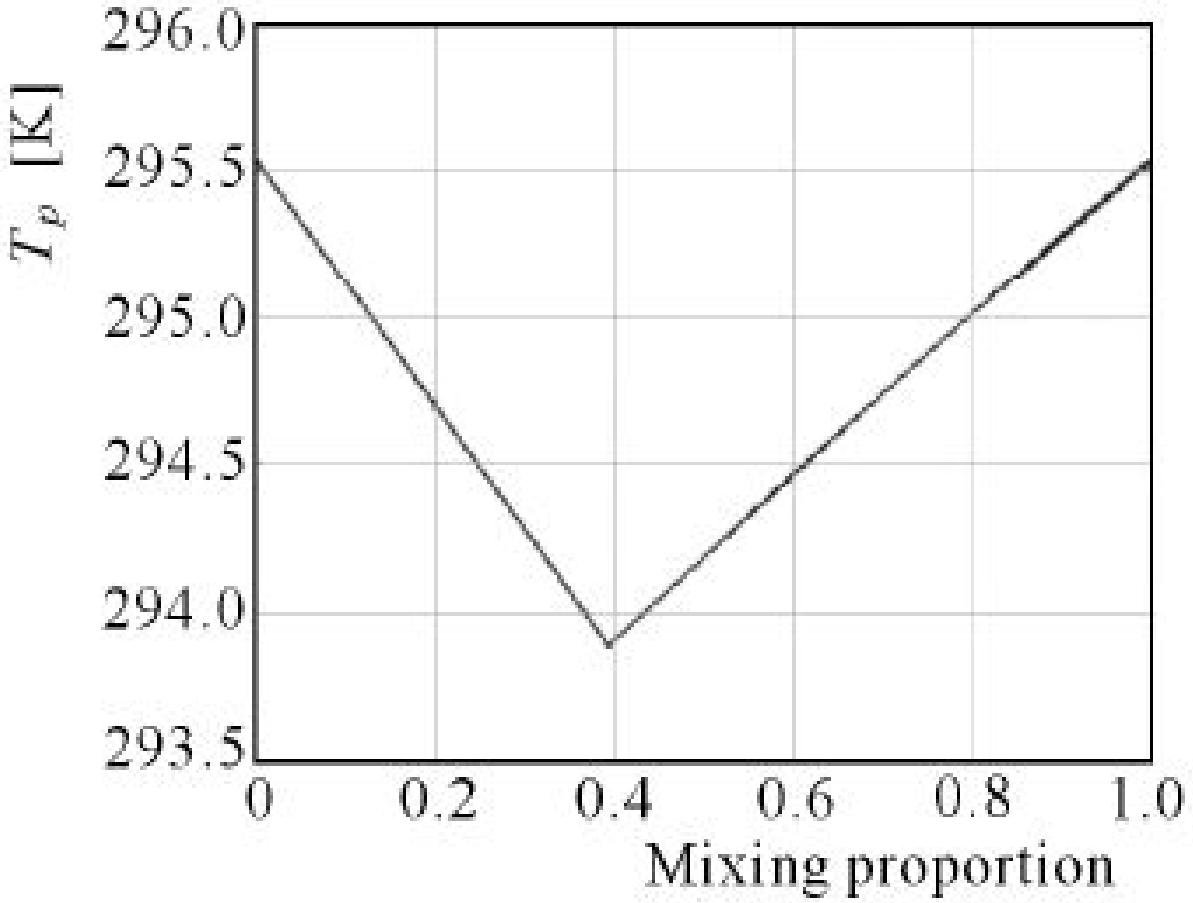

$$B \equiv g\left[\frac{T - T_0}{T_0} + \varepsilon(q_v - q_{v_0}) - q_c\right]$$

Density temperature of a mixture of environmental air of temperature 20.5°C and relative humidity of 70% with saturated cloudy air of temperature 20.1°C and the liquid water mixing ratio 2 g/kg in function of proportion of the environmental air in the mixture.

Consider a bubble of saturated air containing droplets of dia ~10 μm, suspended in a still unsaturated environment. The typical distance between droplets in a cloud is ~ 1mm, terminal fall velocity (Stokes regime) ~ 1mm/s, and typical evaporation time of a small droplet is of the order of 1s.

Assume, that the bubble of zero buoyancy (mean density is the same as environmental) and of temperature equal to that of the environmental air. This is possible, since the density deficit due to humidity (virtual temperature effect) can be compensated by the Liquid Water Content (LWC). In terms of atmospheric thermodynamics, we state that the density temperature of the bubble is the same as the density temperature of the environment.

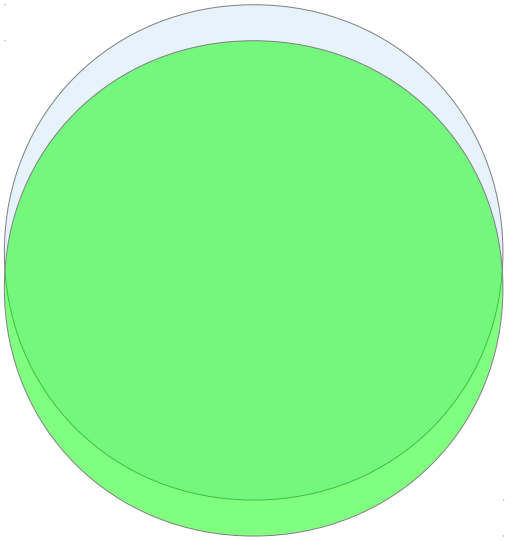

Simplified set of equations of cloud dynamics, thermodynamics and microphysics :

$$D/Dt \equiv \partial/\partial t + \mathbf{v}\cdot\nabla$$

$$B \equiv g\left[\frac{T - T_0}{T_0} + \varepsilon(q_v - q_{v_0}) - q_c\right], \qquad (2)$$

$$\frac{D\mathbf{v}}{Dt} = -\nabla\pi + \mathbf{k}B + \nu\nabla^2\mathbf{v}, \qquad (1a)$$

$$\nabla\cdot\mathbf{v} = 0, \qquad (1b)$$

$$\frac{DT}{Dt} = \frac{L}{c_p}C_d + \mu_T\nabla^2 T, \qquad (1c)$$

$$\frac{Dq_v}{Dt} = -C_d + \mu_v\nabla^2 q_v, \qquad (1d)$$

$$\frac{Dq_c}{Dt} = C_d. \qquad C_d = \int f\frac{dm}{dt}\,dr, \qquad \frac{D^* f}{D^* t} = -\frac{\partial}{\partial r}\left(f\frac{dr}{dt}\right) + \eta,$$

$$D^*/D^*t \equiv \partial/\partial t + (\mathbf{v} - \mathbf{k}v_t)\cdot\nabla$$

Andrejczuk et al., 2004

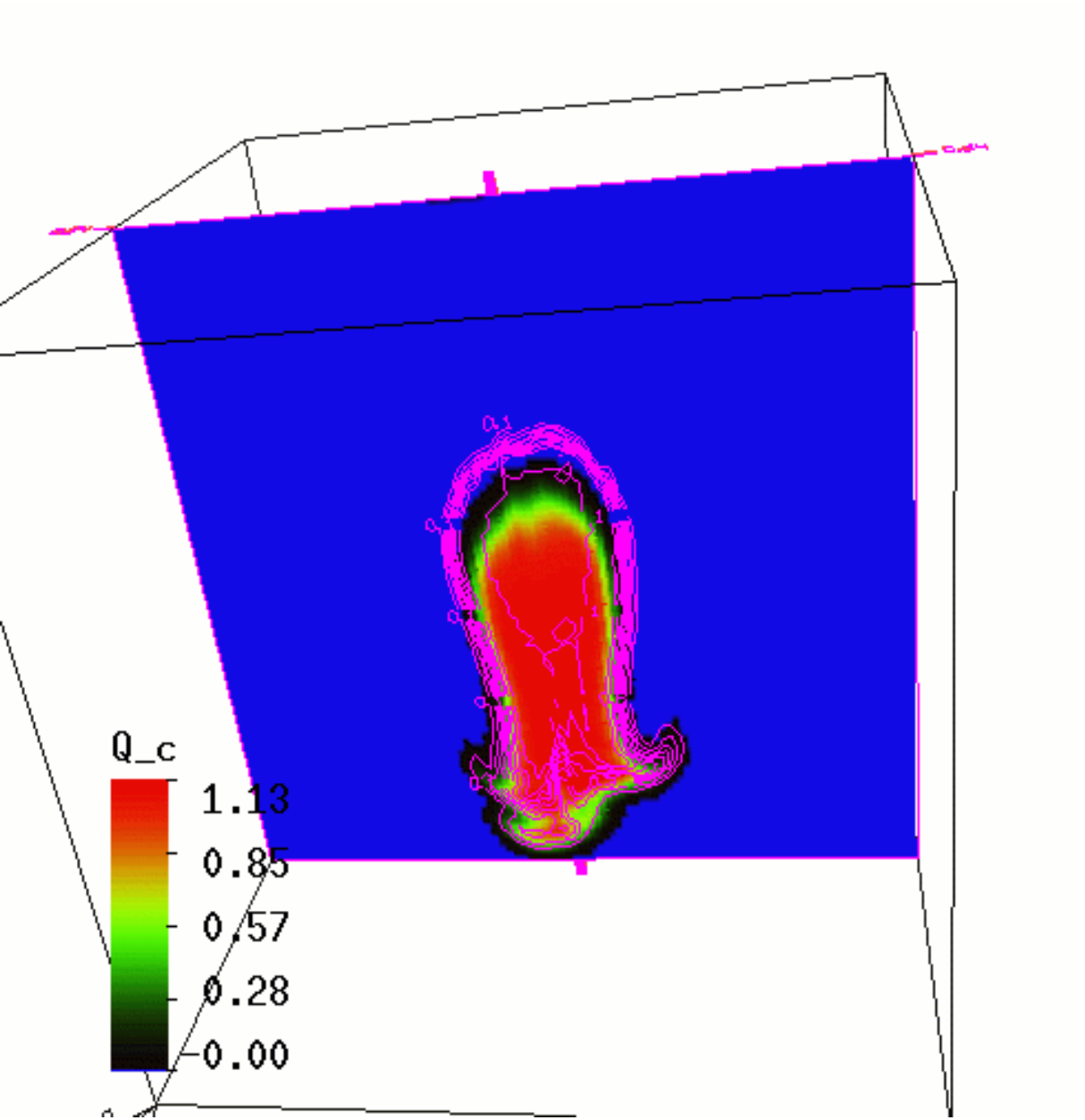

Liquid water content on a vertical cut through three-dimensional thermal containing cloud droplets after 13s of the model time. Model domain: 1x1x1m, 100x100x100 gridpoints, fully cyclic boundary conditions. 16 classes of droplets, sedimentation accounted for.

Isolines represent passive scalar. Initial conditions: thermal at rest with zero buoyancy, unsaturated environment.

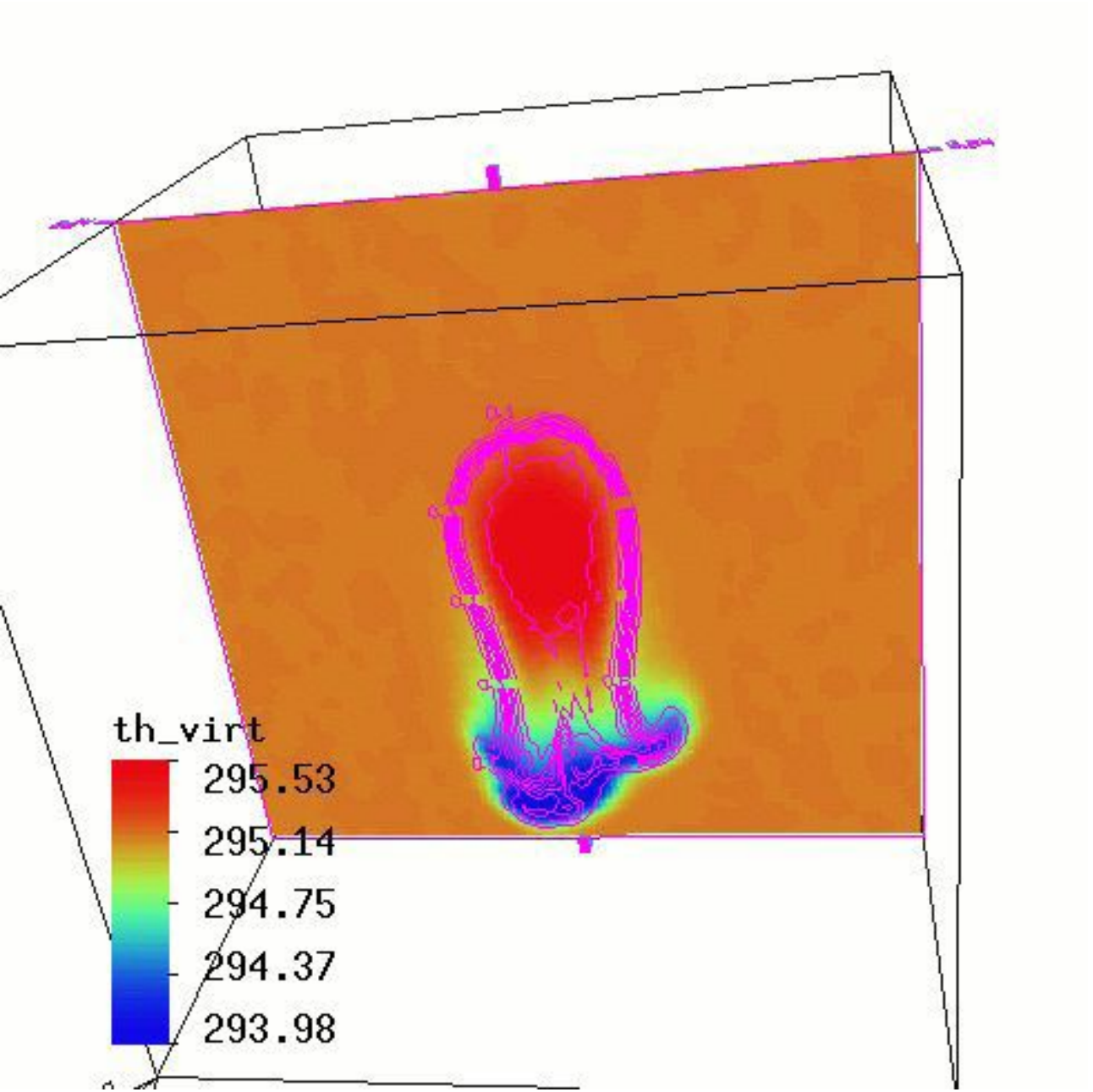

Virtual potential temperature,
the most interesting feature is a maximum of the evaporative cooing due to droplet sedimentation in the bottom of the thermal

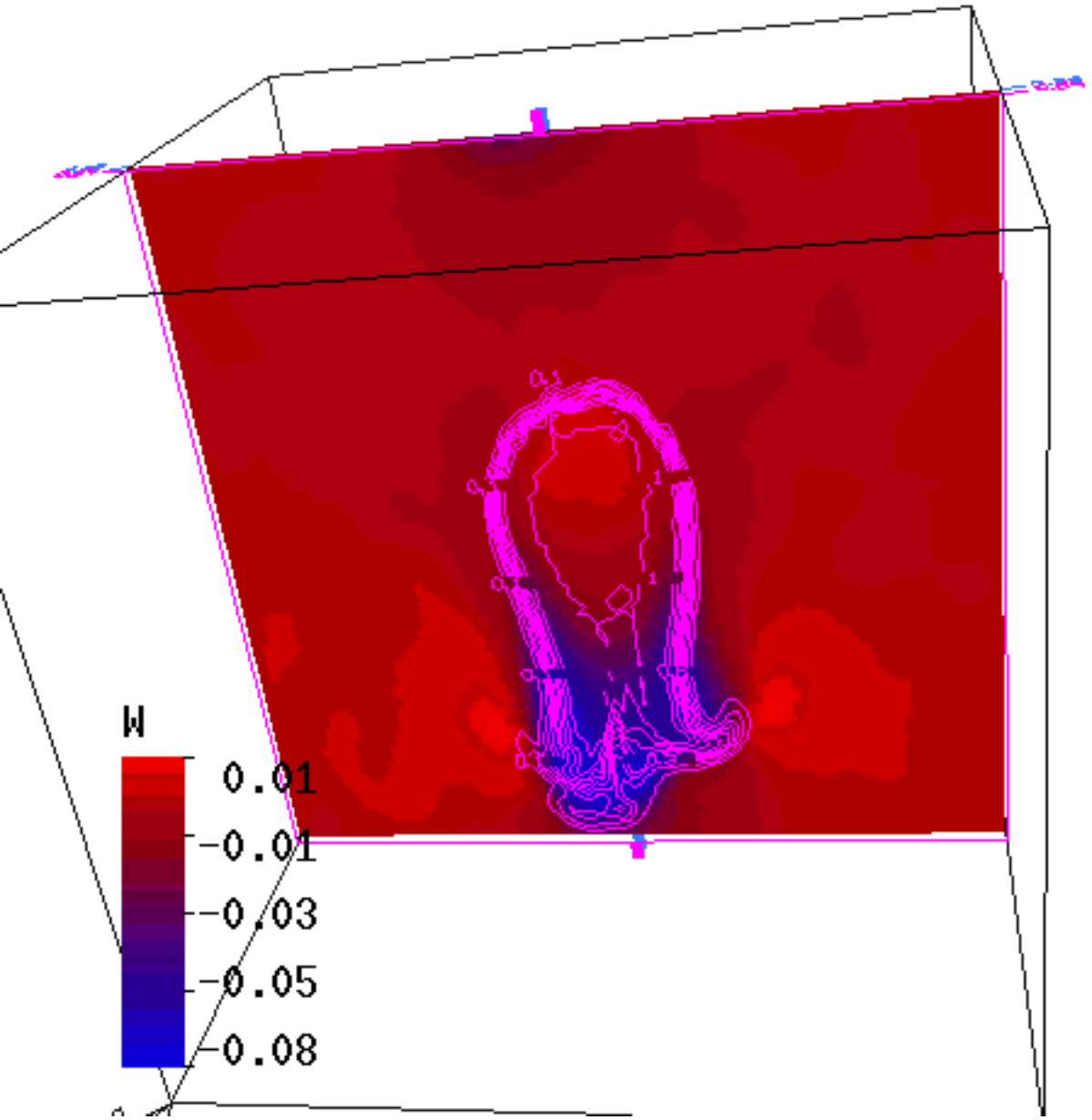

Vertical velocity. Maximum of the downward velocity is spatially correlated with the mimimum of the virtual potential temperature.

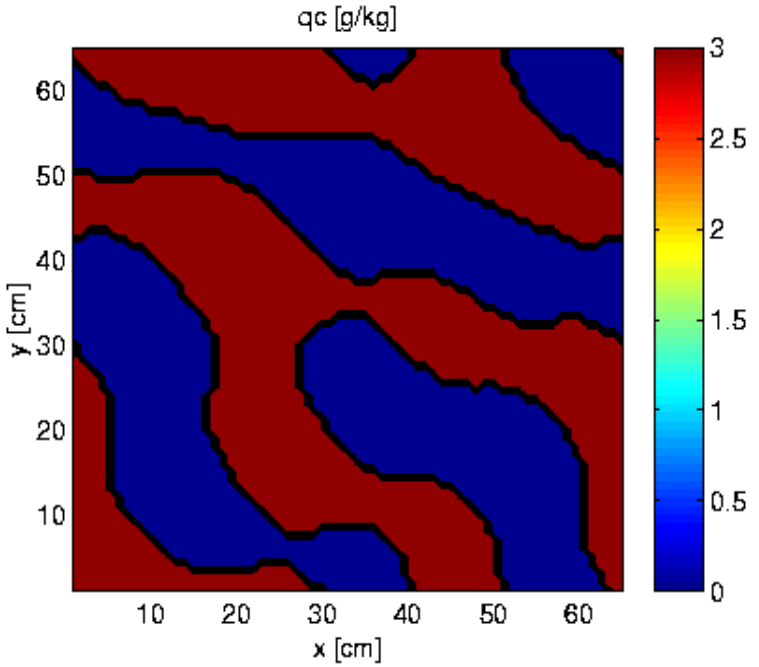

Initial conditions for more realistic simulation of cloud-clear air mixing.

(Andrejczuk et al., 2004)

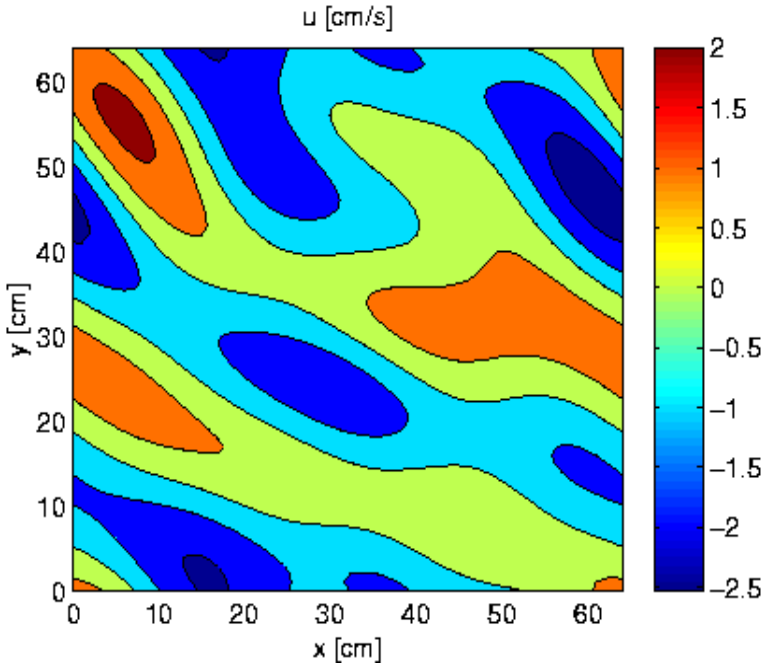

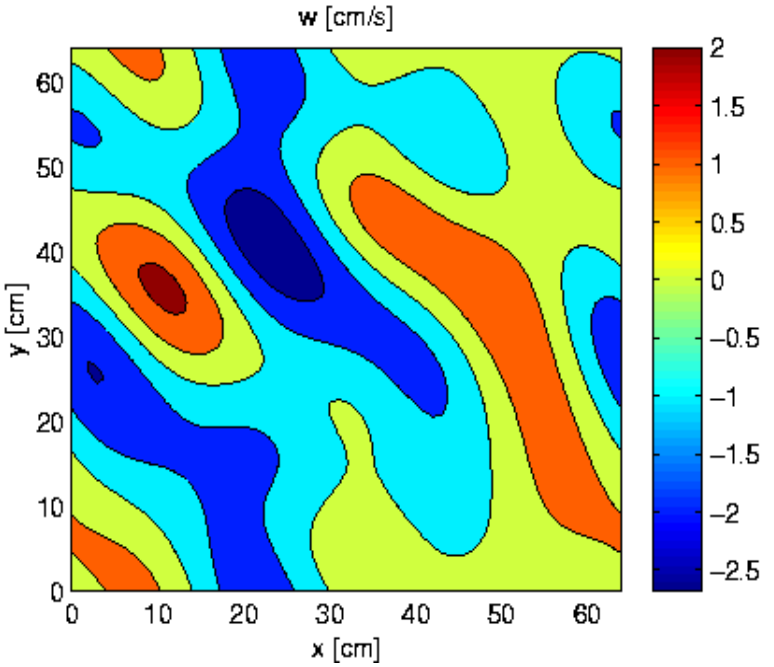

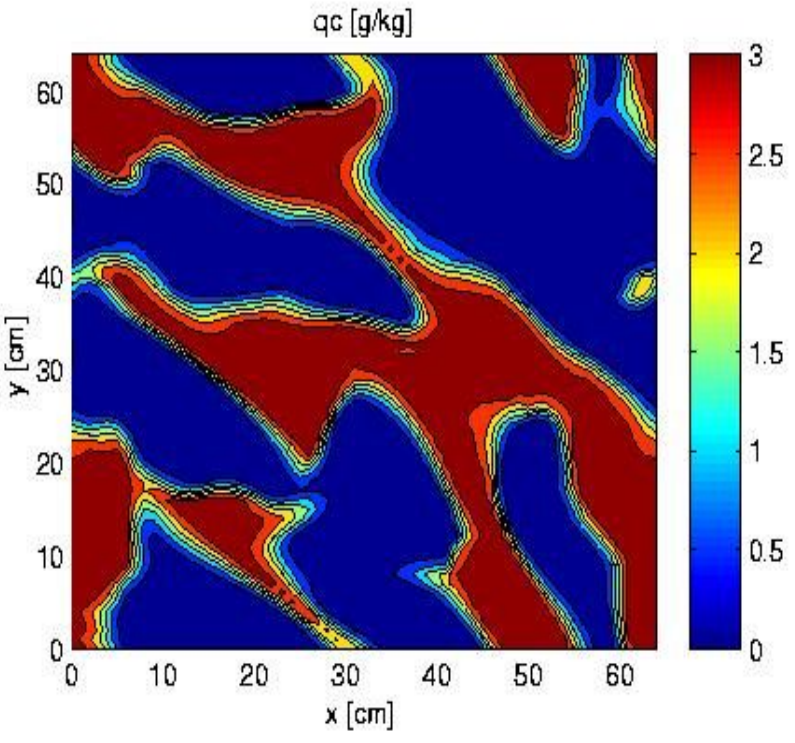
qc [g/kg]
y [cm]
x [cm]
0
10
20
30
40
50
60
3
2.5
2
1.5
1
0.5
0

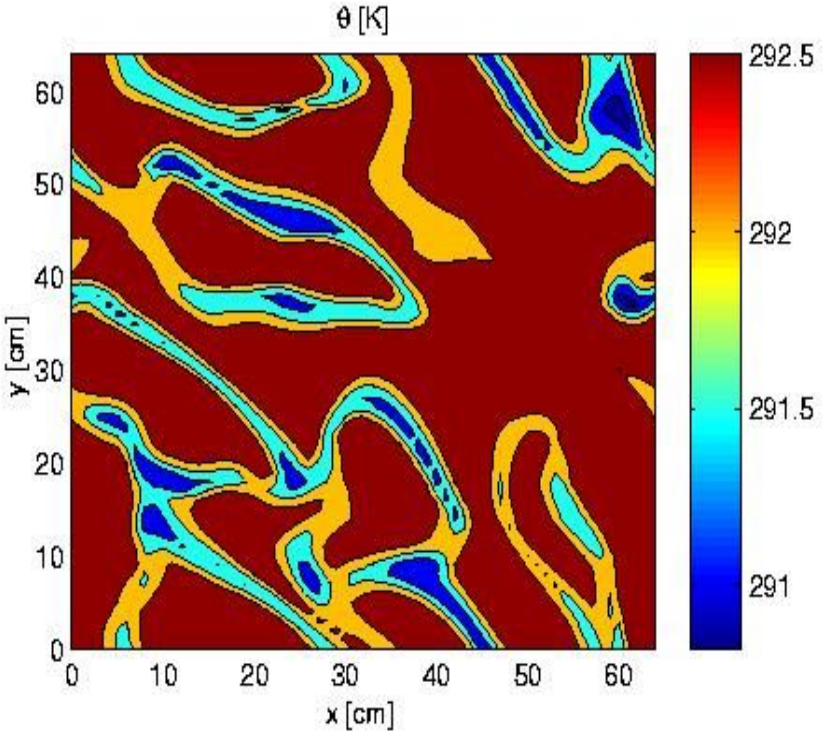
θ [K]
y [cm]
x [cm]
0
10
20
30
40
50
60
292.5
292
291.5
291

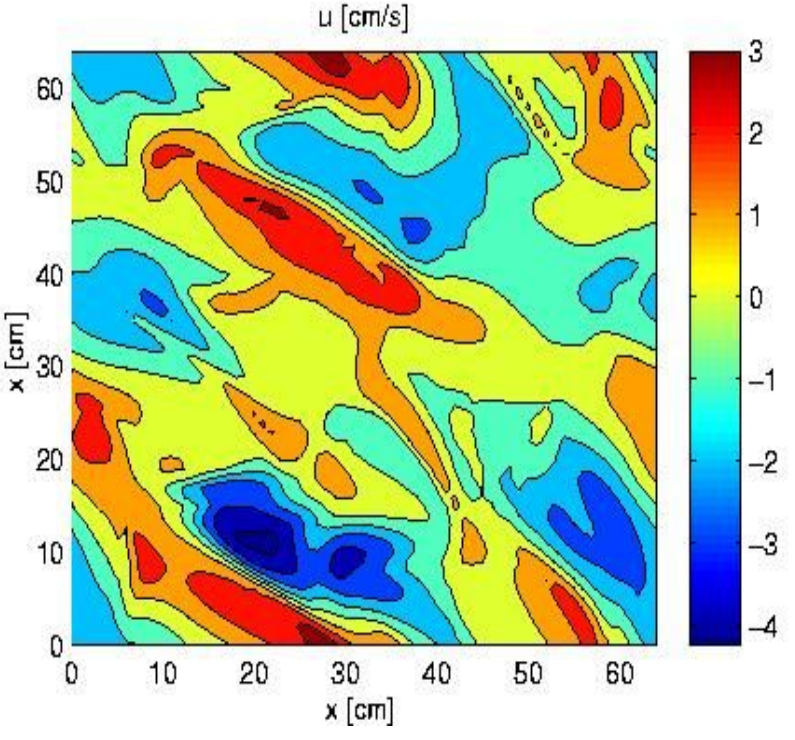
u [cm/s]
x [cm]
x [cm]
0
10
20
30
40
50
60
3
2
1
0
−1
−2
−3
−4

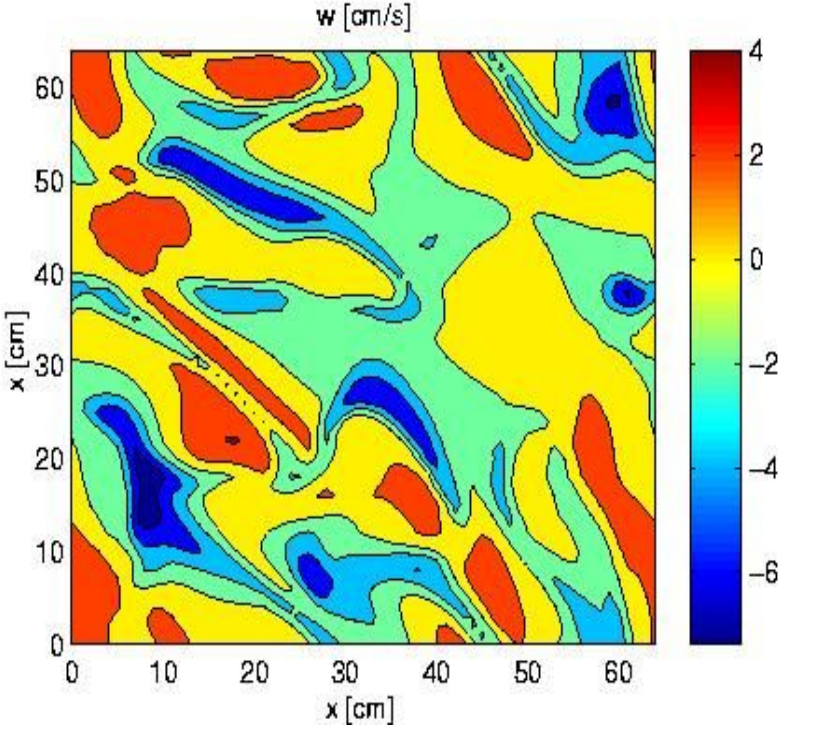
w [cm/s]
x [cm]
x [cm]
0
10
20
30
40
50
60
4
2
0
−2
−4
−6

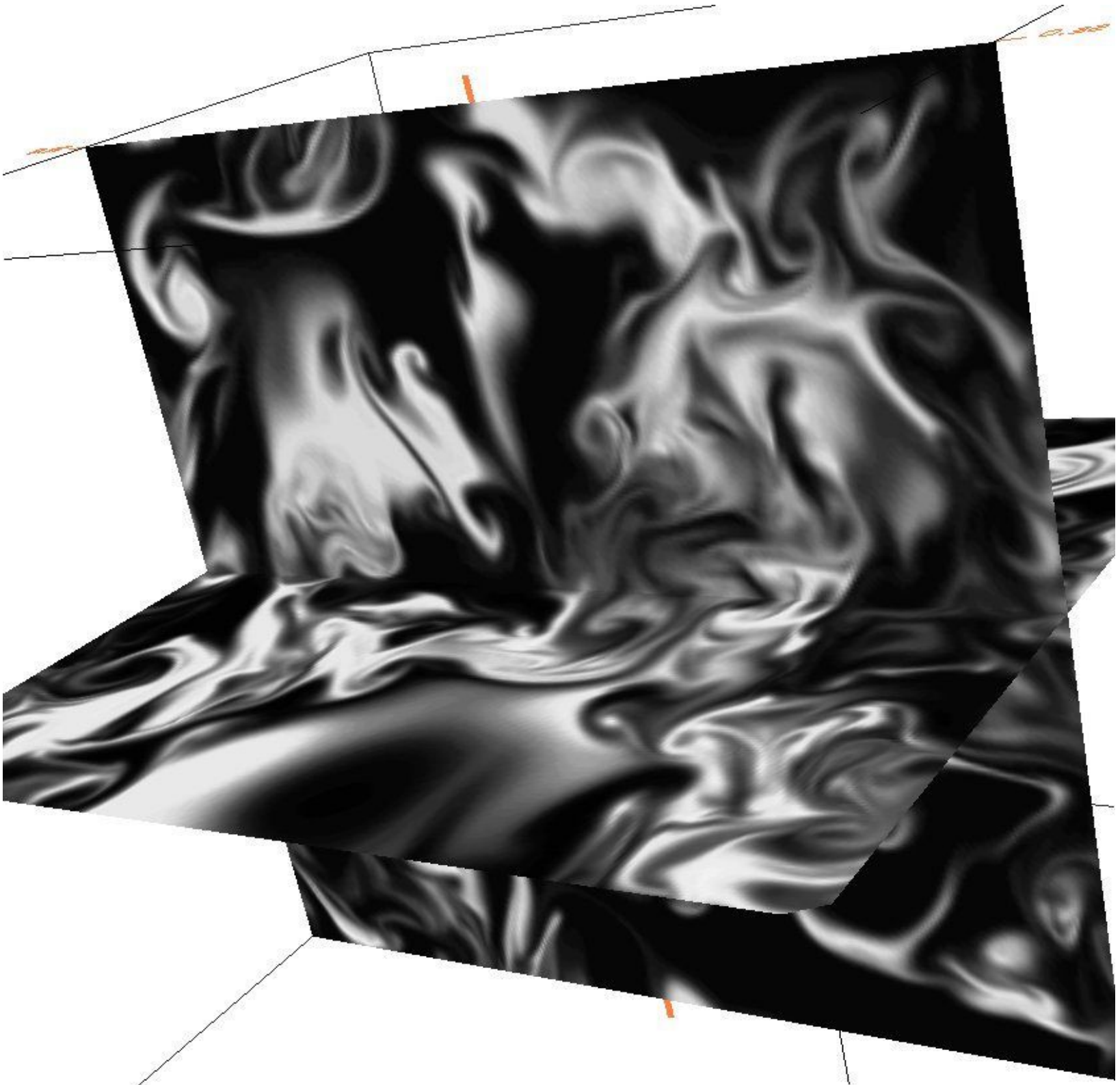

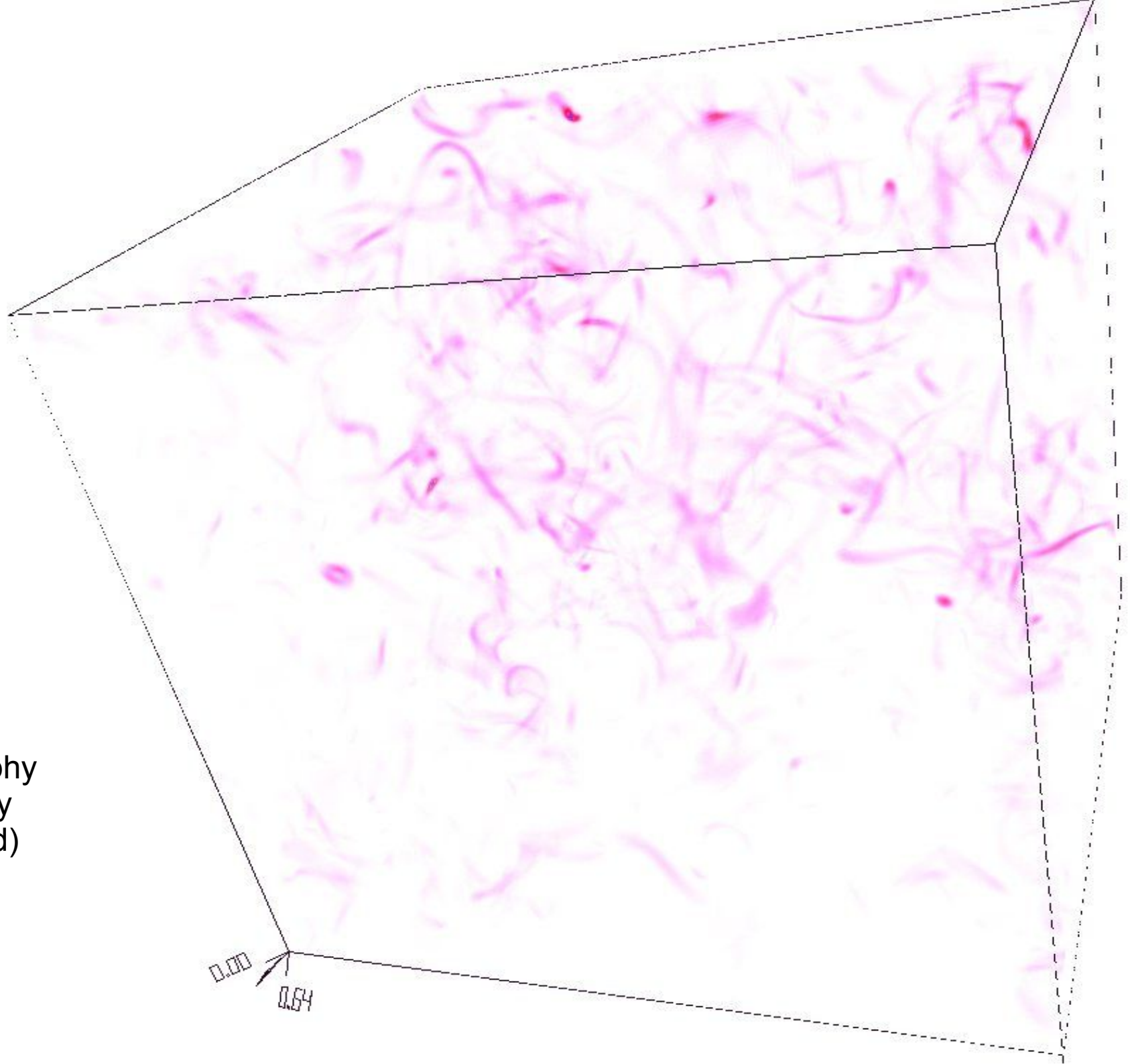

Enstrophy (vorticity squared)

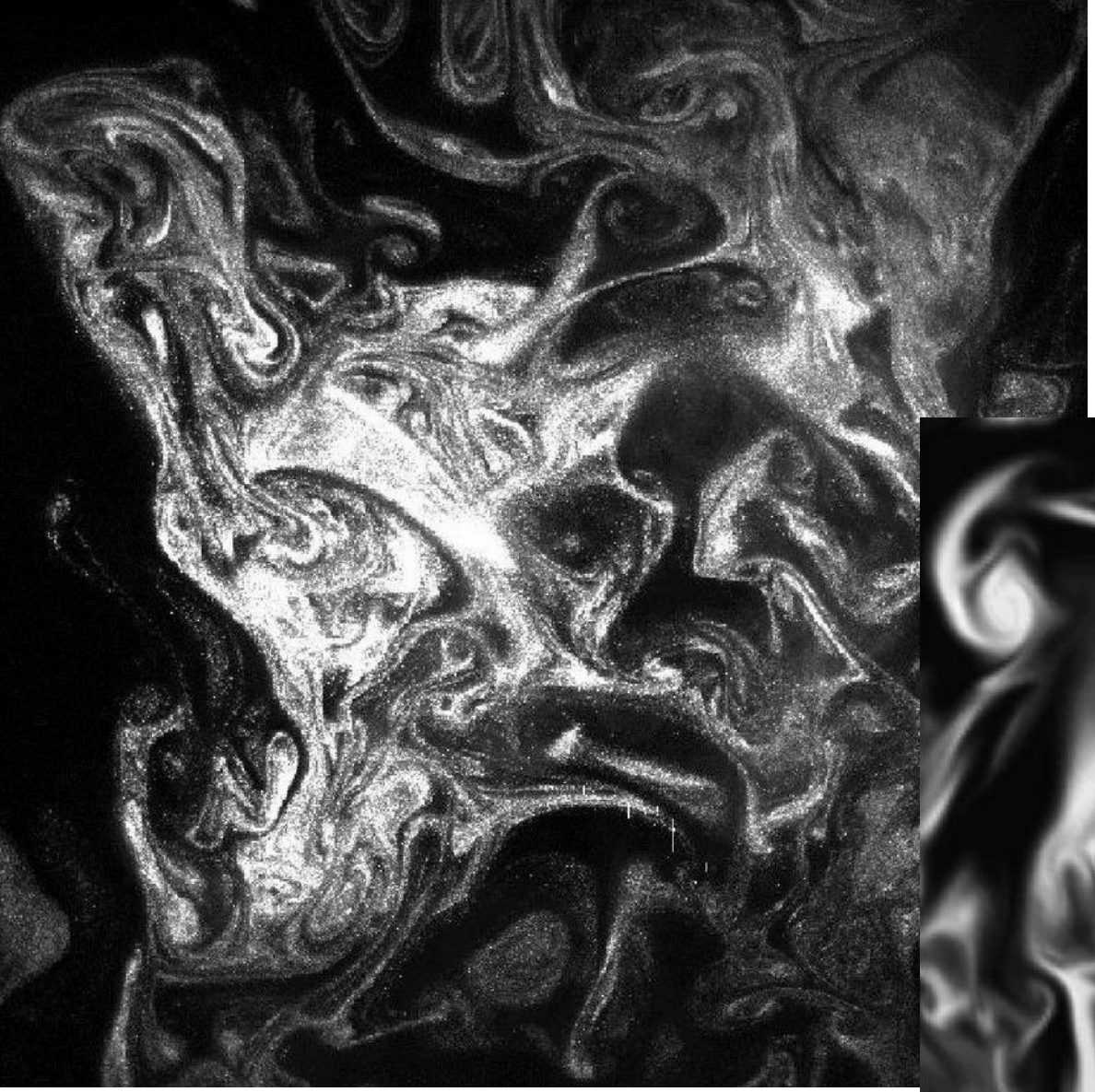

Mixing inside cloud chamber vs.
numerical simulation.

TABLE 1. Characteristic parameters for three flow configurations. The entries in the table are the Taylor microscale Reynolds number Re_λ, initial value of the TKE, the maximum TKE dissipation rate ϵ_{max}, the maximum velocity, the minimum Kolmogorov length scale η_{min}, and the eddy mixing time scale τ_T.

Group	Re_λ	TKE ($m^2\ s^{-2}$)	ϵ_{max} ($m^2\ s^{-3}$)	$\max\|u\|$ (10^{-2} m s^{-1})	η_{min} (10^{-3} m)	τ_T (s)
High	553	2.16×10^{-2}	7.2×10^{-3}	59.2	0.8	0.5
Moderate	276	5.40×10^{-3}	1.1×10^{-3}	29.6	1.3	0.9
Low	55	2.16×10^{-4}	4.4×10^{-4}	5.92	1.7	1.3

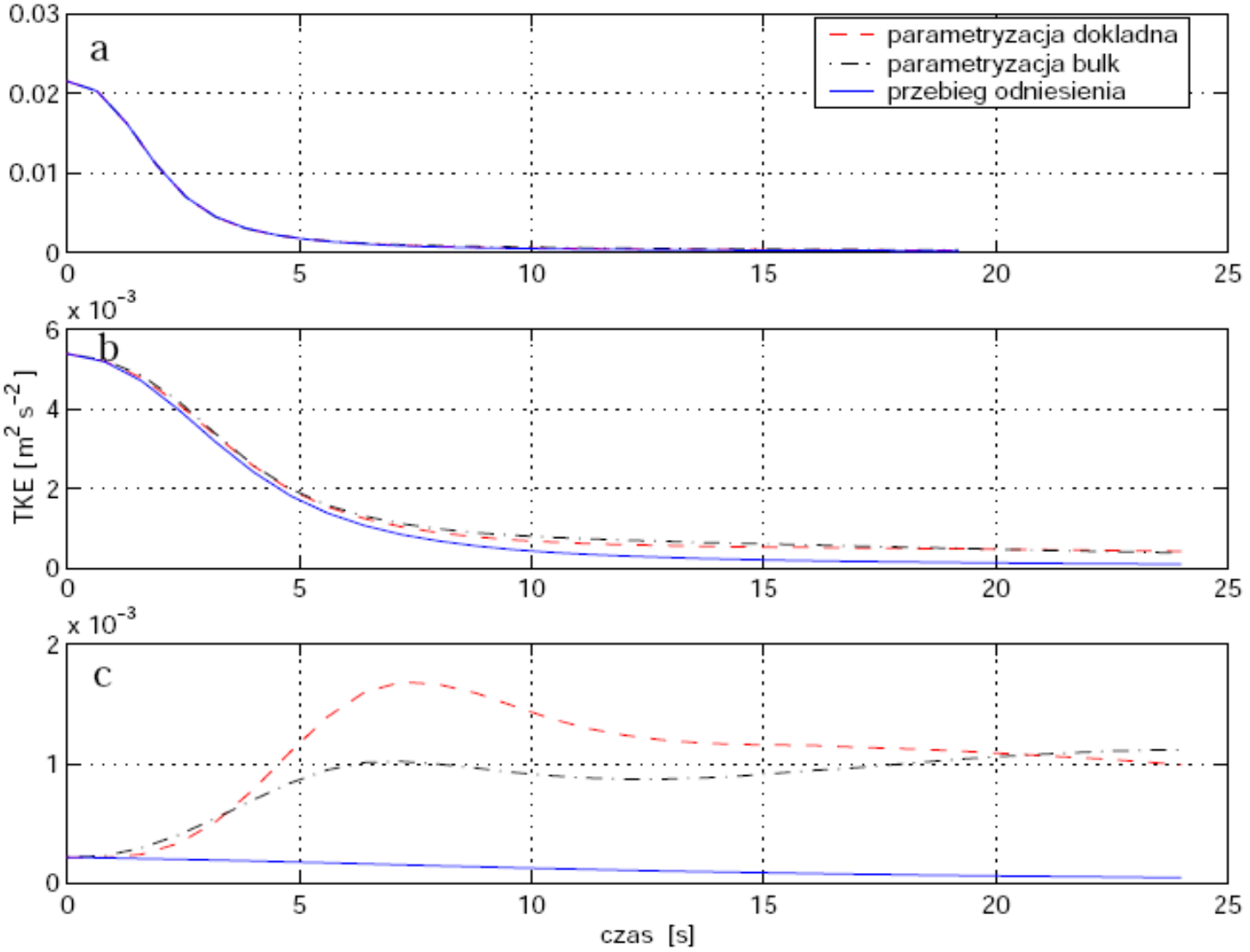

Evolution of TKE in all simulations. (top) high-, (middle) moderate-, and (bottom) low-TKE input.

Solid lines are for dry reference runs (decaying TKE), while dashed and dashed–dotted lines are for detailed and bulk microphysics, respectively.

Andrejczuk et al., 2004, 2006.

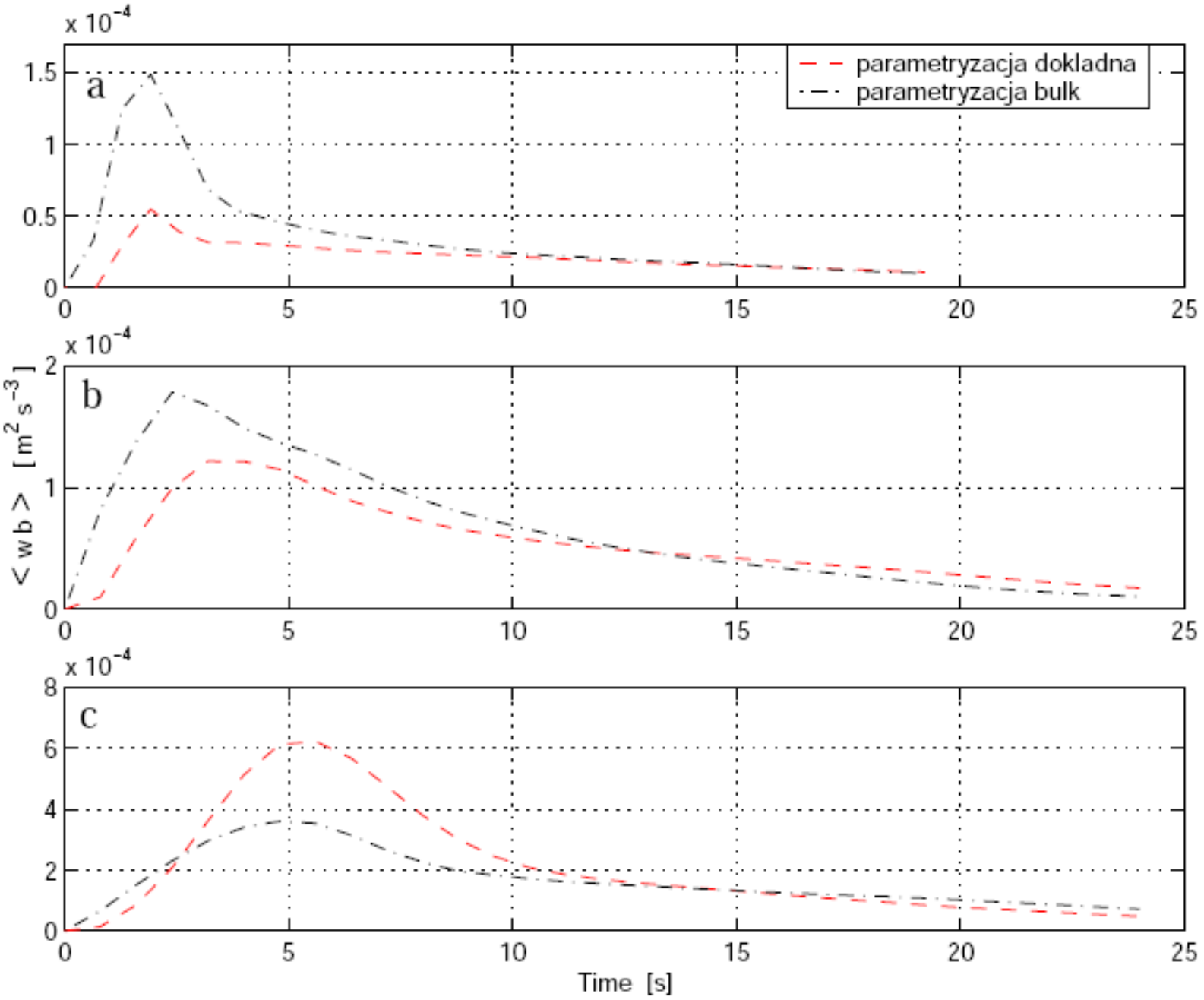

Evolution of TKE production by buoyancy forces in all simulations; (top) high-, (middle) moderate-, and (bottom) low-TKE input. Dashed and dashed–dotted lines are for detailed and bulk microphysics, respectively.

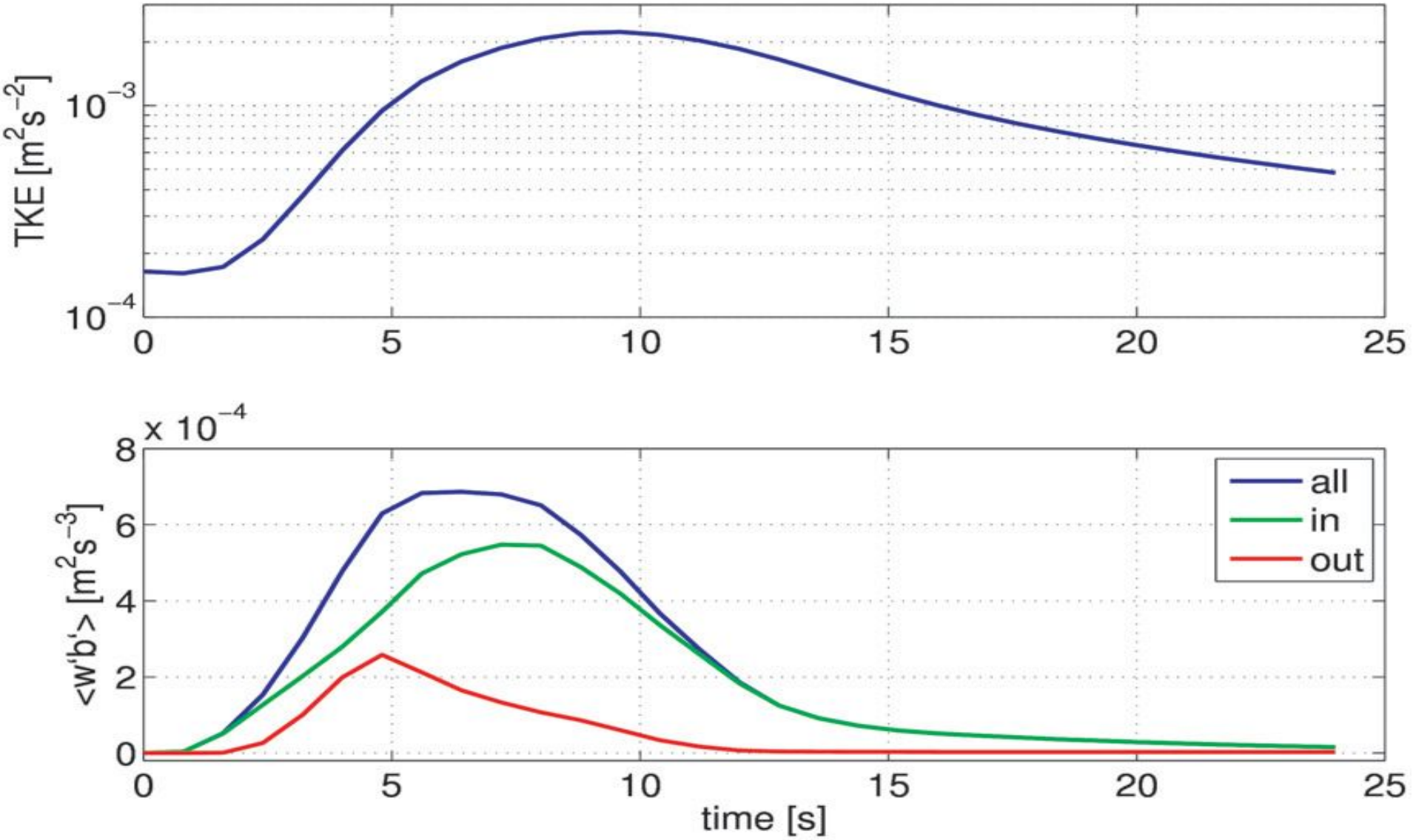

Evolution of the volume-averaged TKE (upper panel) and its buoyant production (lower panel, blue line); contributions to the buoyant production by buoyancy fluctuations within and outside the limits resulting from isobaric and adiabatic mixing are shown in green and red lines, respectively.

Malinowski et al., 2008

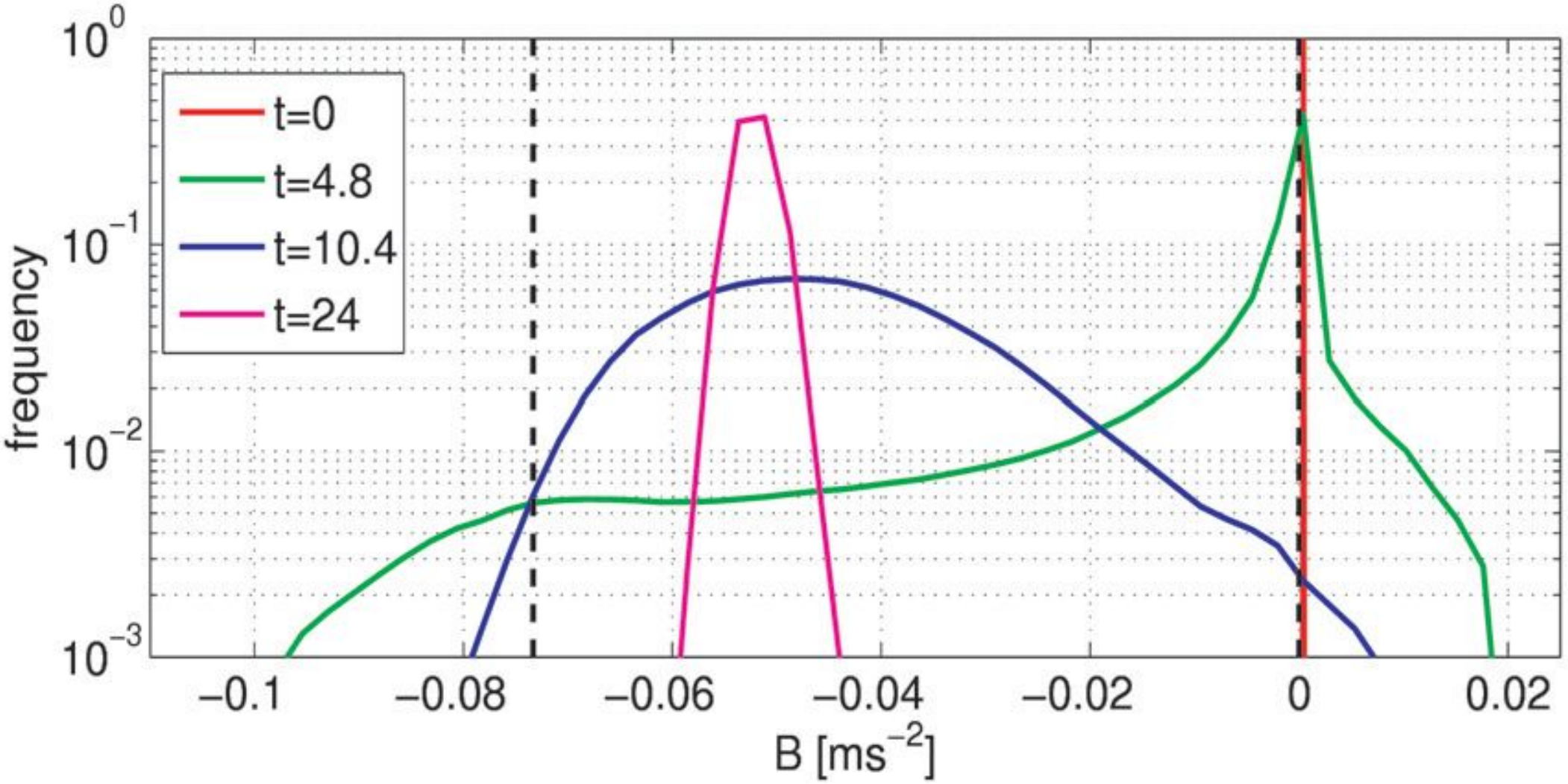

Histograms of buoyancy within the model domain at the beginning of calculations and at times of 4.8, 10.4 s and at the end of calculations (24 s). Dashed black lines show the range of buoyancy fluctuations due to isobaric and adiabatic mixing.

Simplified set of equations of cloud dynamics, thermodynamics and microphysics :

$$D/Dt \equiv \partial/\partial t + \mathbf{v}\cdot\nabla$$

$$B \equiv g\left[\frac{T - T_0}{T_0} + \varepsilon(q_v - q_{v_0}) - q_c\right], \qquad (2)$$

$$\frac{D\mathbf{v}}{Dt} = -\nabla\pi + \mathbf{k}B + \nu\nabla^2\mathbf{v}, \qquad (1a)$$

$$\nabla\cdot\mathbf{v} = 0, \qquad (1b)$$

$$\frac{DT}{Dt} = \frac{L}{c_p}C_d + \mu_T\nabla^2 T, \qquad (1c)$$

$$\frac{Dq_v}{Dt} = -C_d + \mu_v\nabla^2 q_v, \qquad (1d)$$

$$\frac{Dq_c}{Dt} = C_d. \qquad C_d = \int f\frac{dm}{dt}\,dr, \qquad \frac{D^* f}{D^* t} = -\frac{\partial}{\partial r}\left(f\frac{dr}{dt}\right) + \eta,$$

$$D^*/D^*t \equiv \partial/\partial t + (\mathbf{v} - \mathbf{k}v_t)\cdot\nabla$$

Andrejczuk et al., 2004

Evolution of mixing, low initial TKE, detailed microphysics:

dependence on the initial liquid water content of cloudy filaments.

Andrejczuk et al., 2006

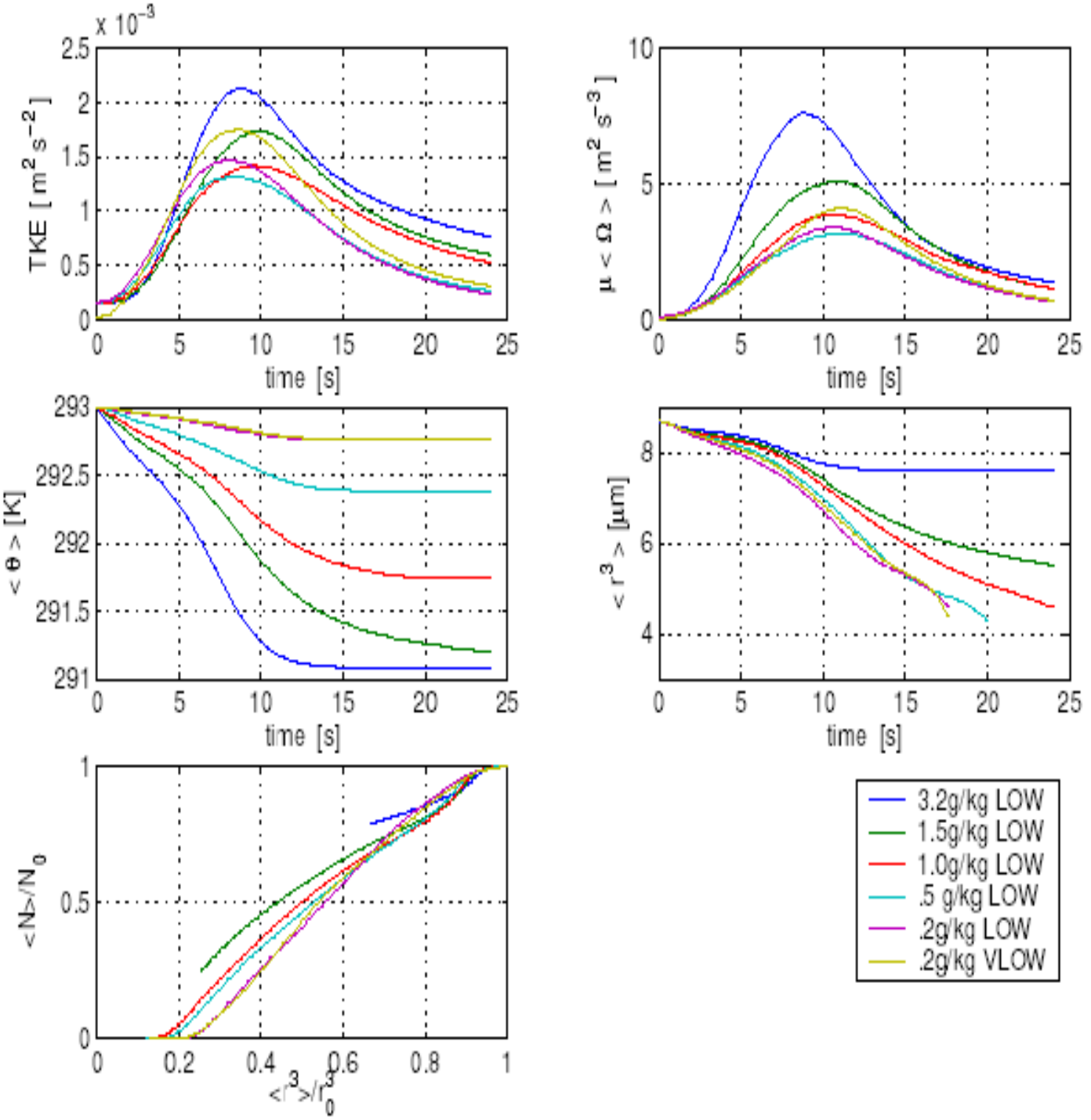

Evolution of mixing, low initial TKE, detailed microphysics:

dependence on the relative humidity of the environment.

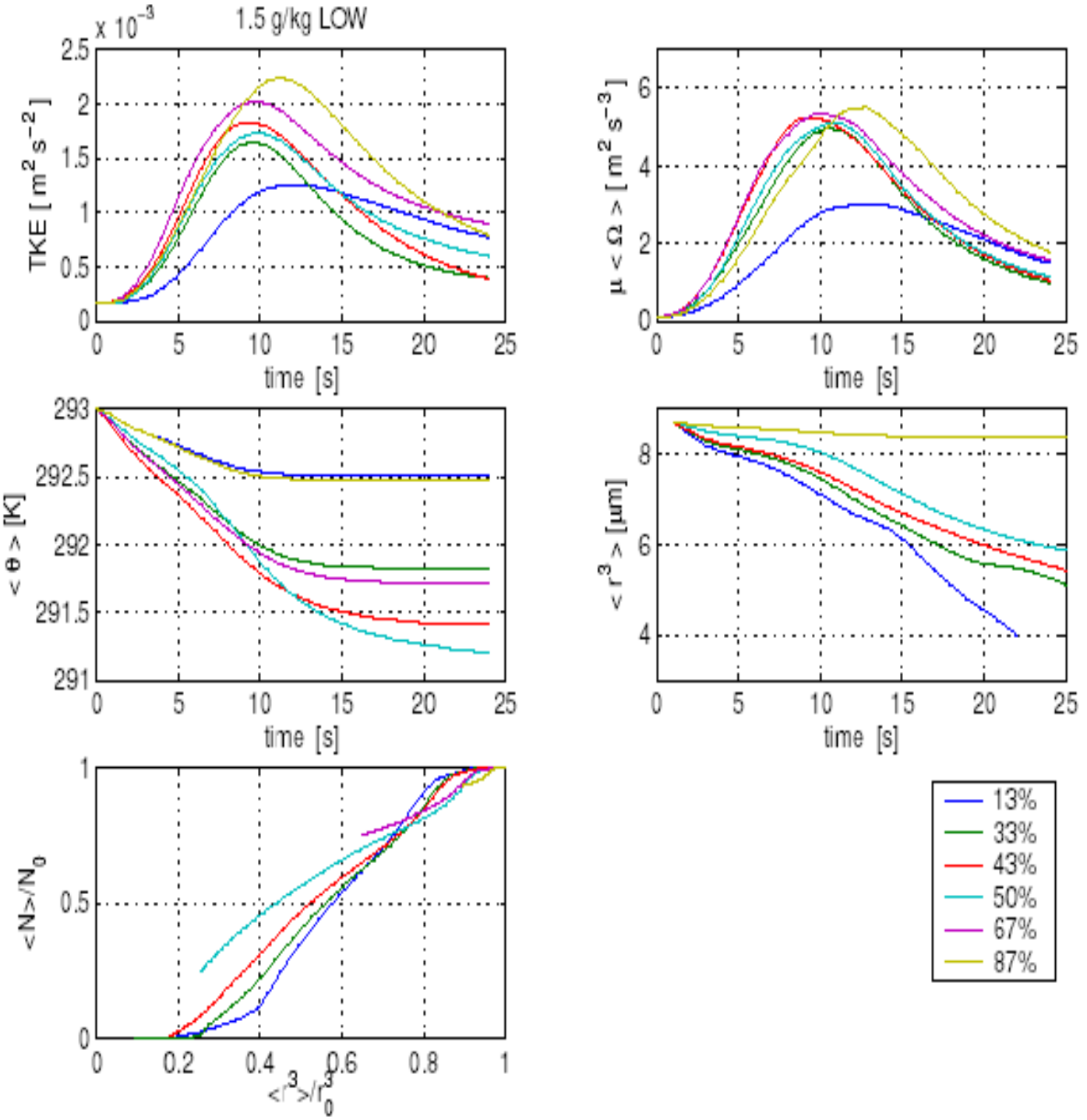

Evolution of mixing, low initial TKE, details microphysics:

dependence on the terminal velocity of cloud droplets.

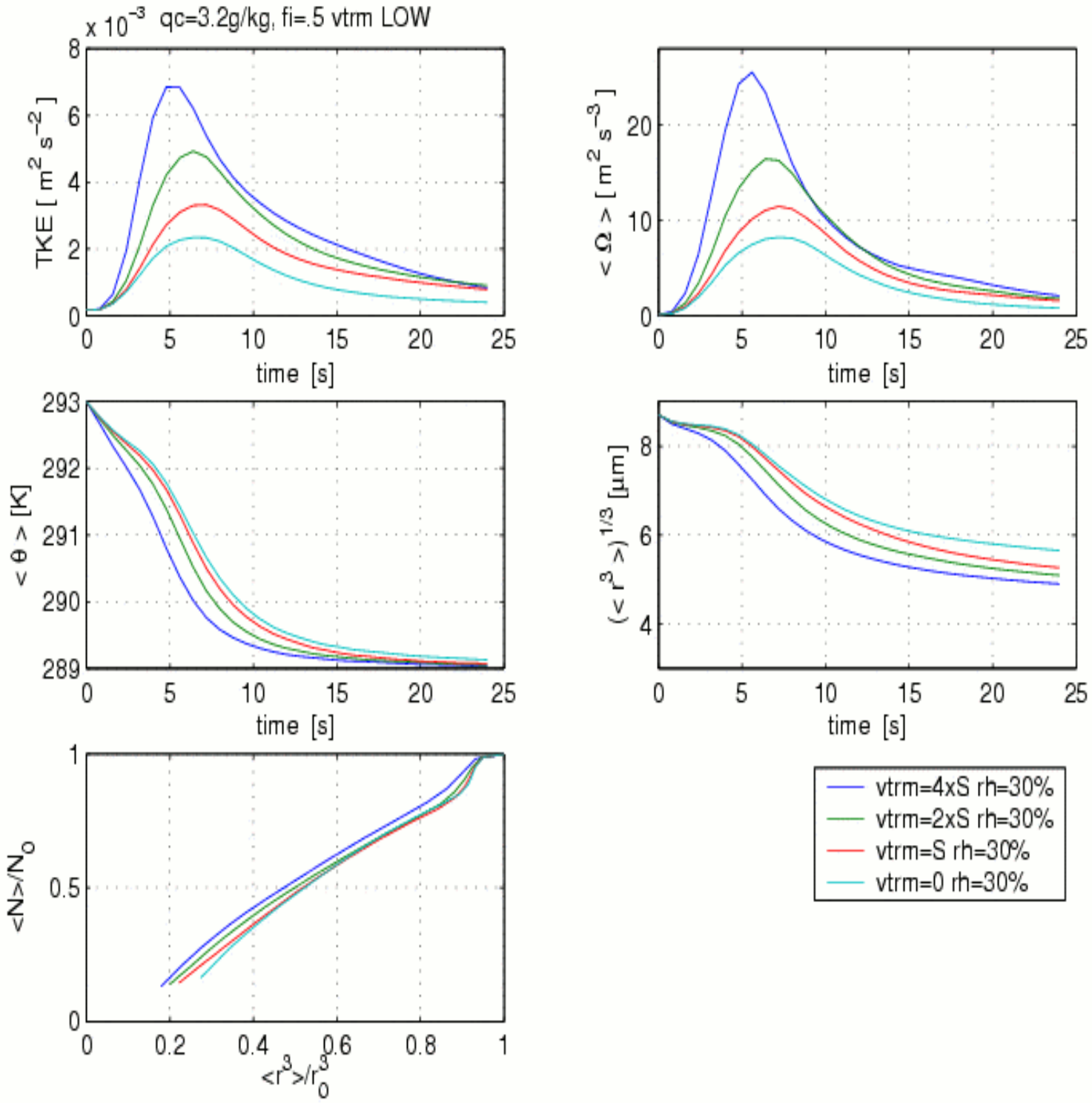

Evolution of mixing, low initial TKE, detailed microphysics:

dependence on the rate of evaporation.

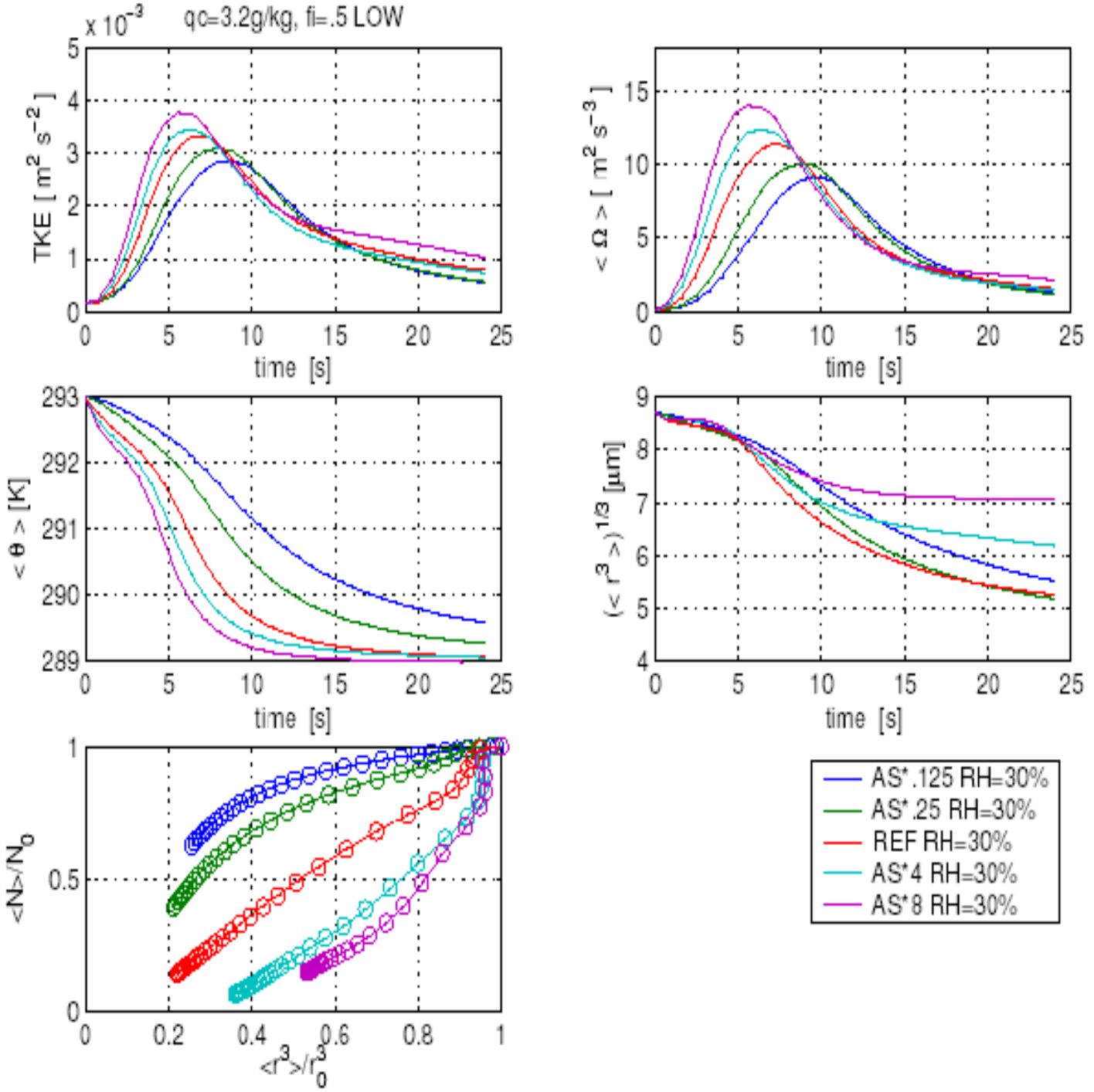

Histograms of velocity fluctuations at 4.8s, 10.4,s 15.2s and at the end of the simulation.

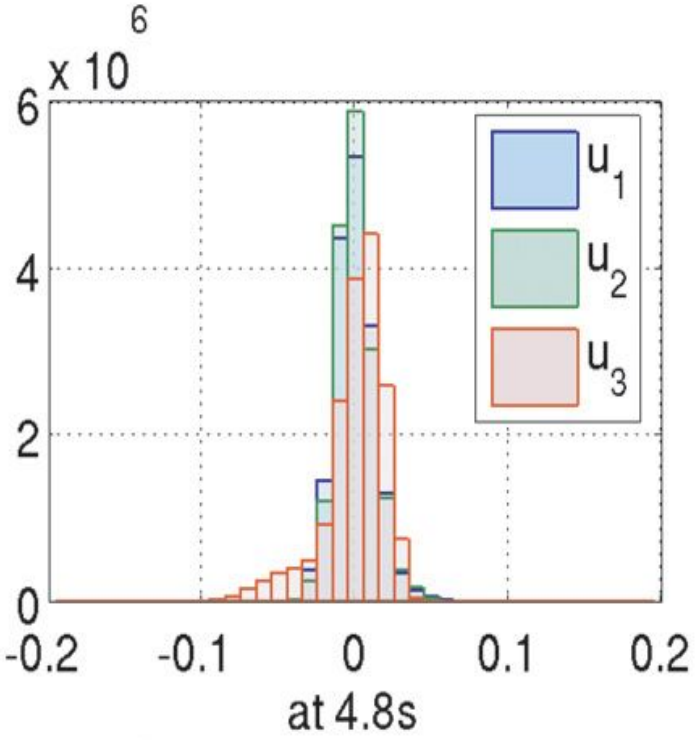

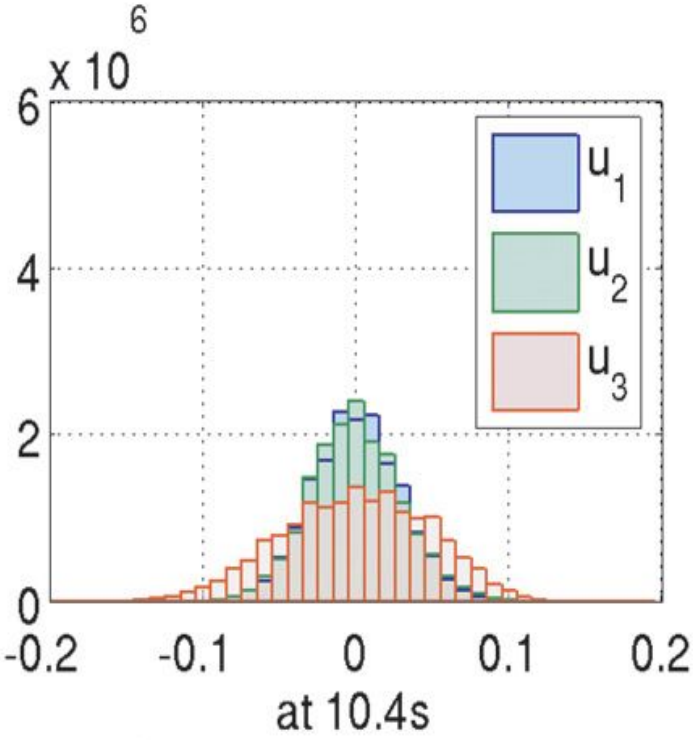

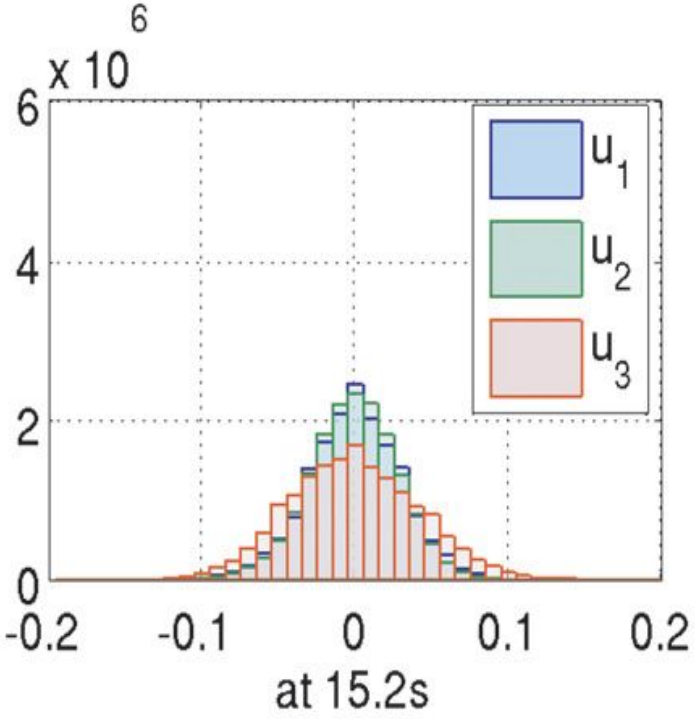

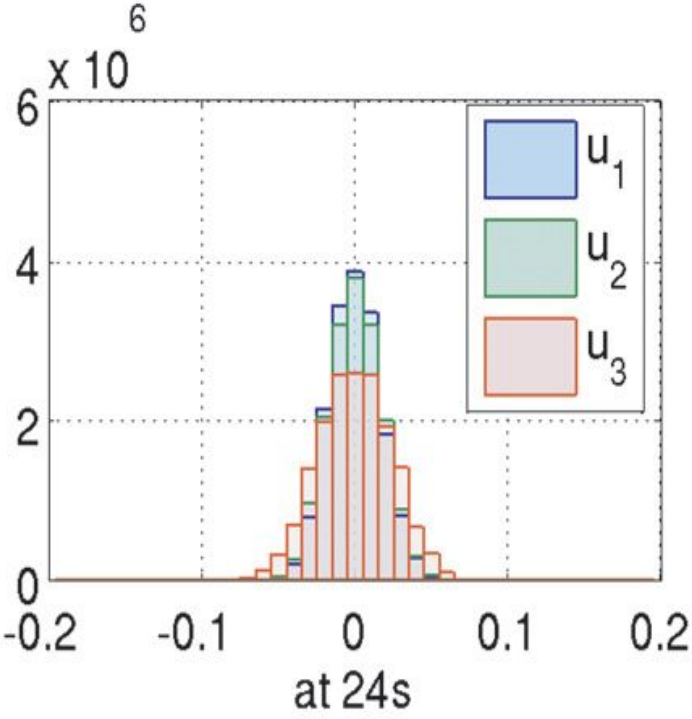

“Passive” cloud chamber:

the set-up of the experiments is designed to mimic basic aspects of small-scale turbulent mixing of a cloudy air with unsaturated environment.

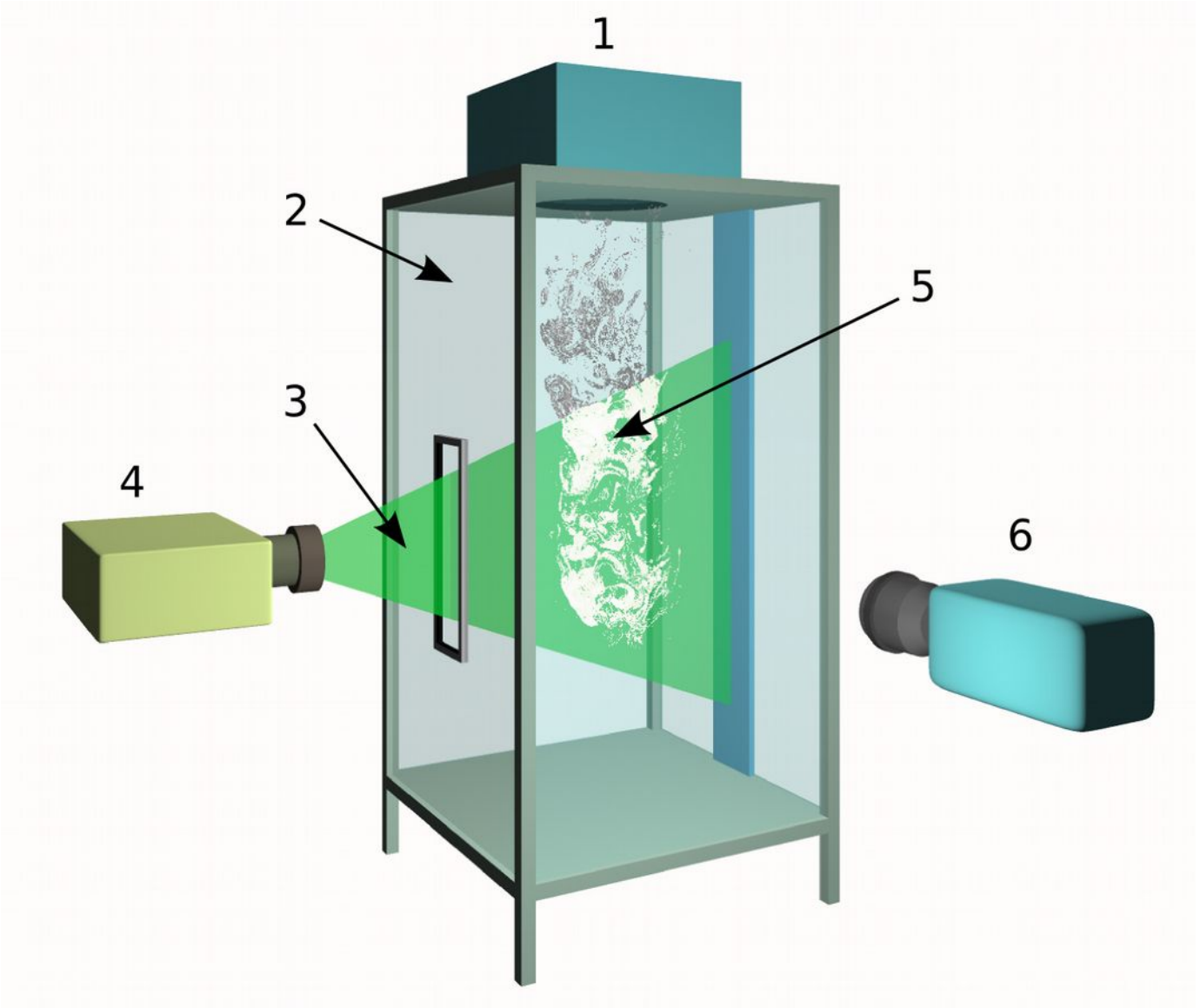

Schematic view of the experimental setup.
1 – box with the droplet generator; 2-cloud chamber; 3 – light sheet; 4 – pulsed laser, 5 – cloudy plume, 6 - camera.

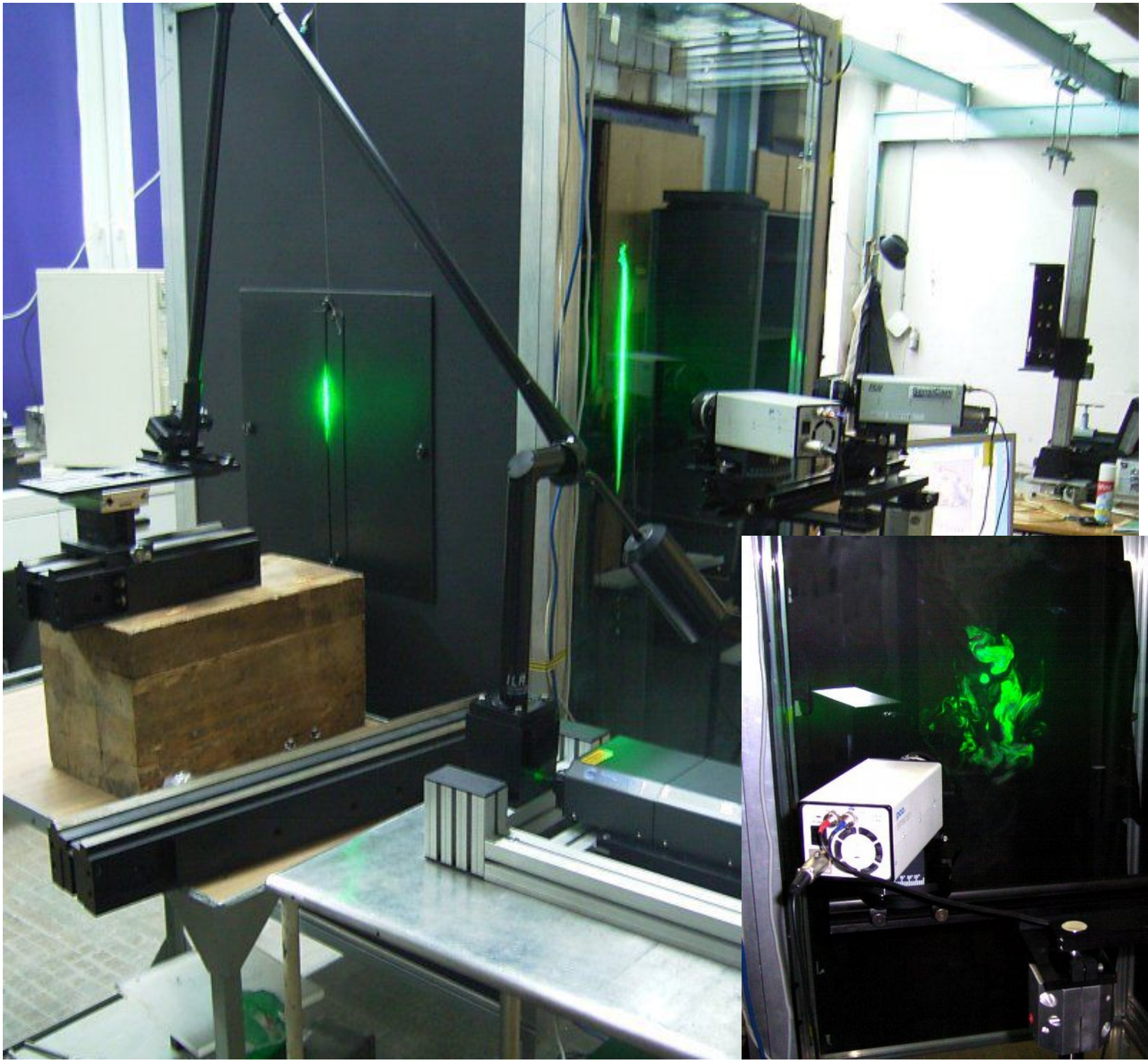
SensiCam

PIV – Particle Imaging Velocimetry

Principle: two consecutive frames compared;displacement of patterns and known time interval between the frames allow to determine velocity in the plane of the light sheet.

A special algorithm developed:

- iterative (with the increasing resolution) correlation of patterns;
- mean motion removal;
- iterative deformation of patterns;
- median filtering.

Result:

benchmark scenes show the average accuracy of the displacement detection =0.3 pixel size.

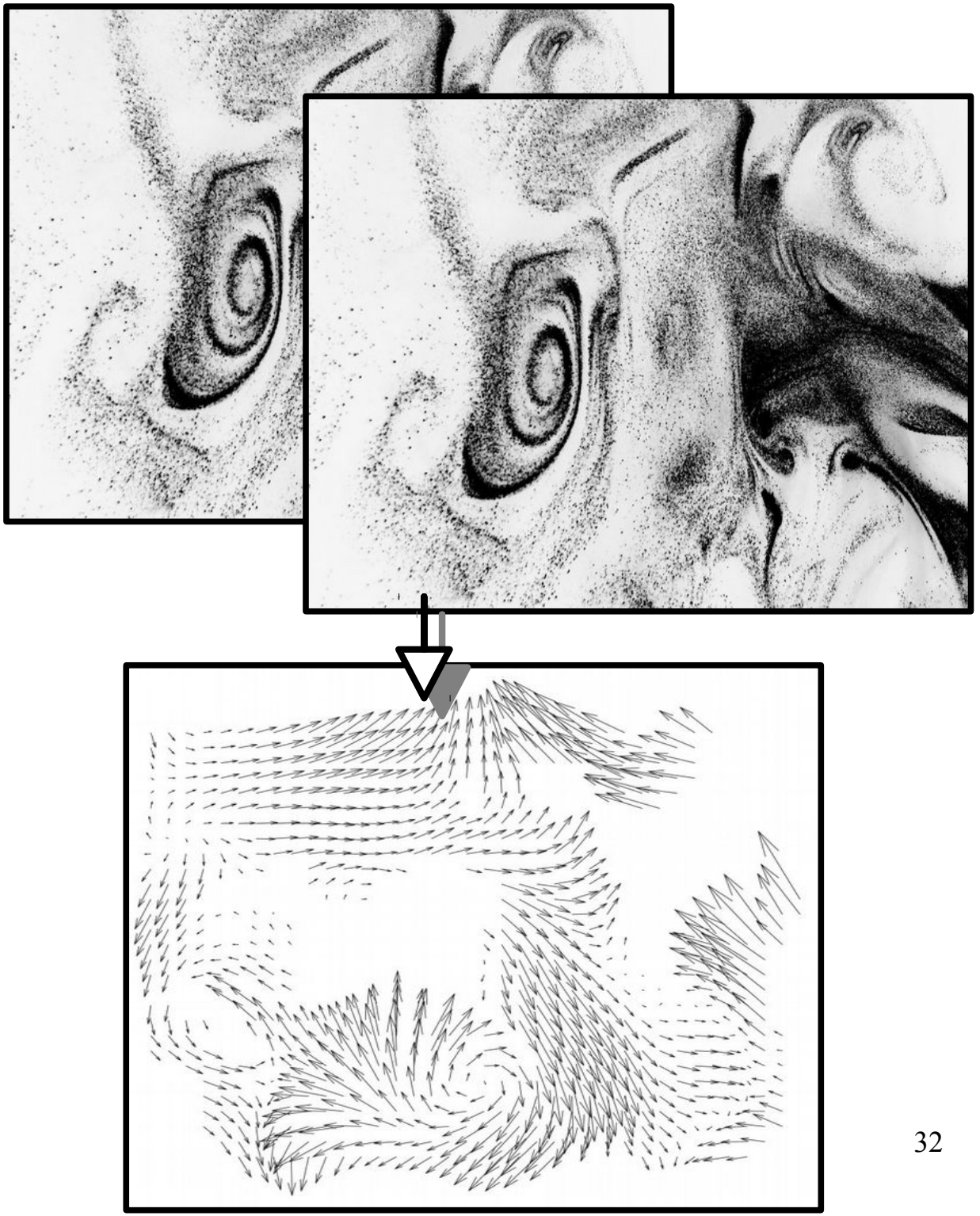

Thermodynamic conditions in the chamber.

LWC in the plume ~24 g/kg .

Plume temperature ~ 25^{o}C, the same as temperature of the unsaturated chamber air.

Relative humidity of the clear air inside the chamber varies in the range 20%~65% for different experiments.

Temperatures and humidities monitored on several levels.

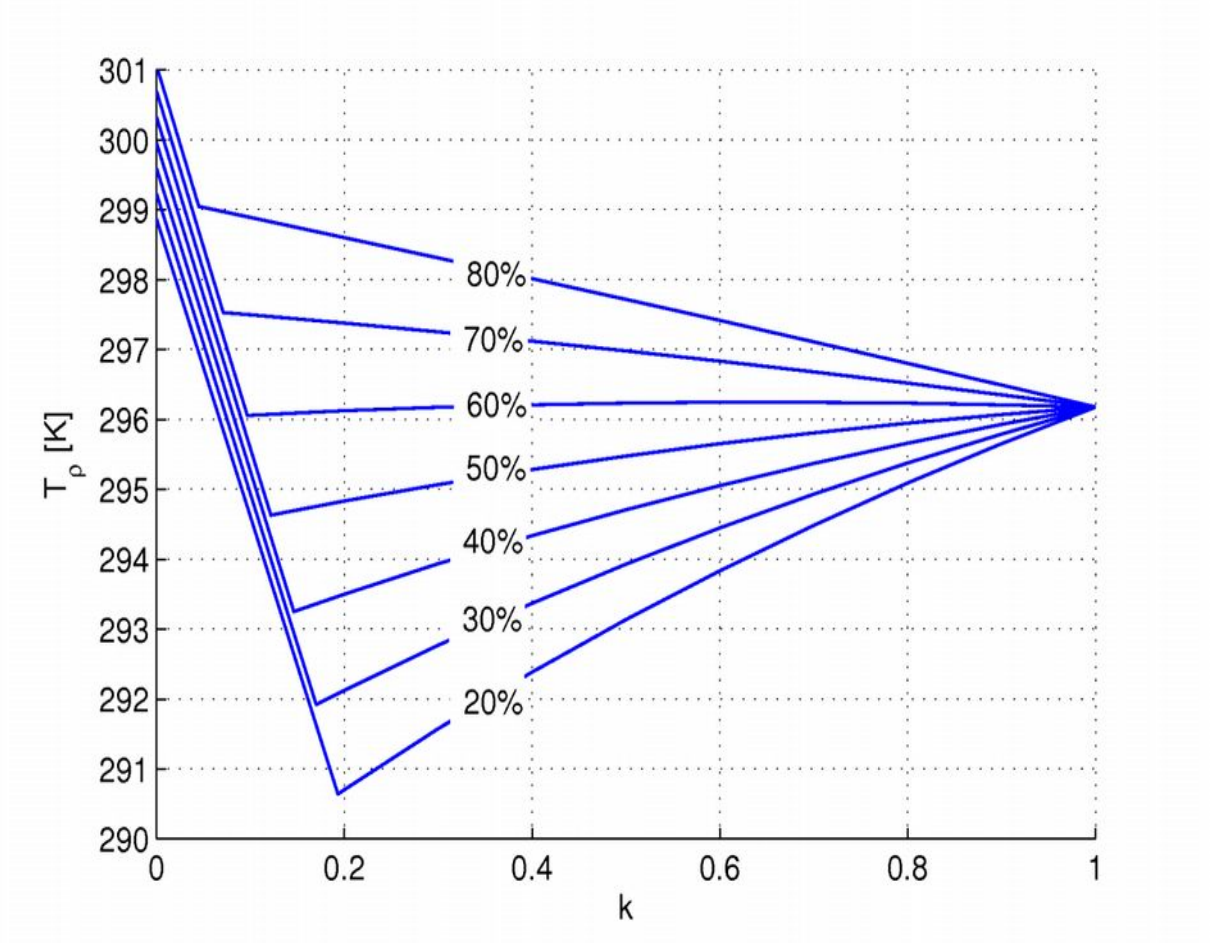

Mixing diagram:
k – fraction of cloudy air in the mixture,
T_ρ – density temperature.

Plume is NEGATIVELY BUOYANT.

Additional negative buoyancy due to evaporative cooling at the edges of cloudy filaments, dominant at ambient humidities less than 60%.

Anisotropy of turbulent velocities
(Malinowski et al., 2008)

Experimental -
average for 20 different runs:

	Std dev. (cm s^{-1})	Skewness	Kurtosis
u_1	**5.4**	−0.01	3.2
u_3	**8.0**	−0.2	3.1

$$(u_1)^2 / (u_3)^2 = \mathbf{0.46 \pm 0.07}$$

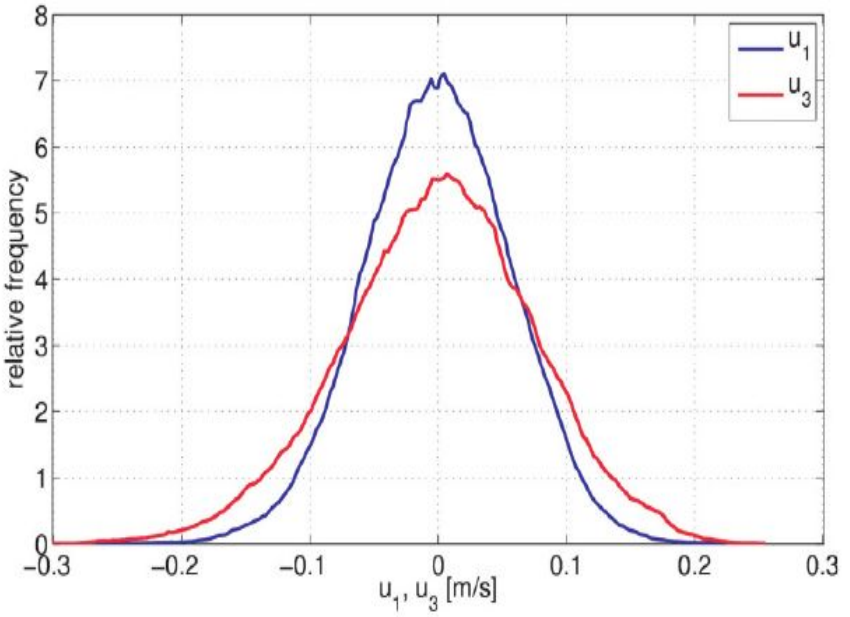

Numerical (LWC 3.2 g/kg):

	Std dev. (cm s^{-1})	Skewness	Kurtosis
u_1	**3,19**	0.01	3.3
u_2	**3,23**	−0.03	3.2
u_3	**4,69**	0.13	2.9

$$(u_{hor})^2 / (u_3)^2 = \mathbf{0.52 \pm 0.07}$$

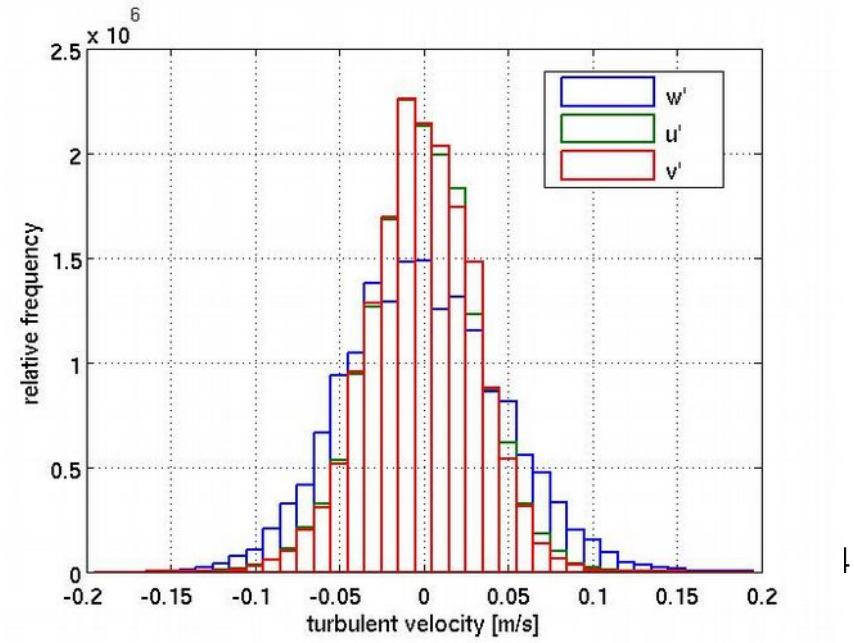

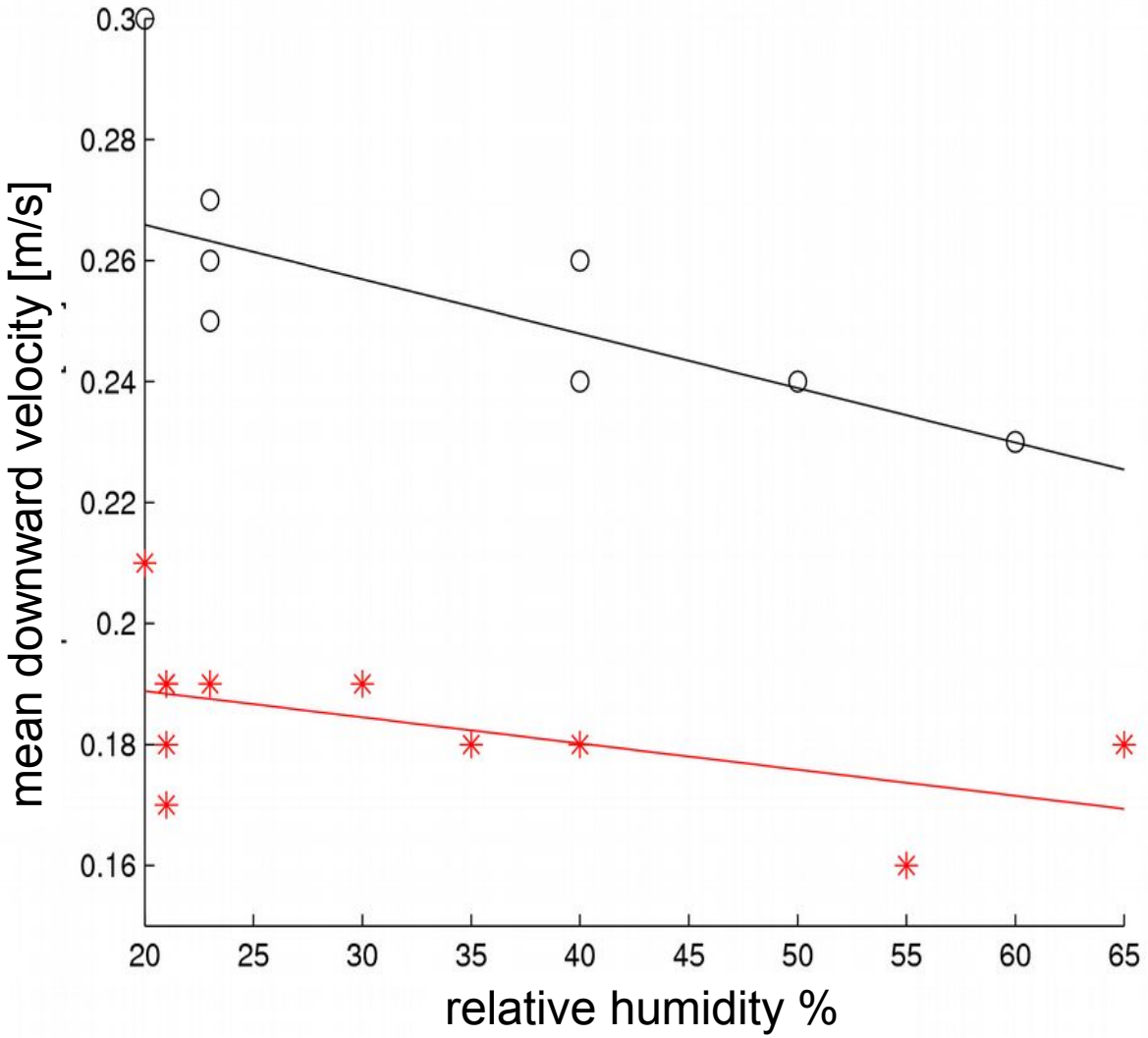

DEHS oil
at 30 cm W=0.025 m/s
at 70 cm W=0.009 m/s

Mean downward velocity of the cloudy plume

black circles – 30 cm down from the inlet;

red stars – 70 cm down from the inlet.

Interpretation:

less evaporative cooling – lower downward velocity;

more entrained environmental air – lower downward velocity due to dilution of momentum.

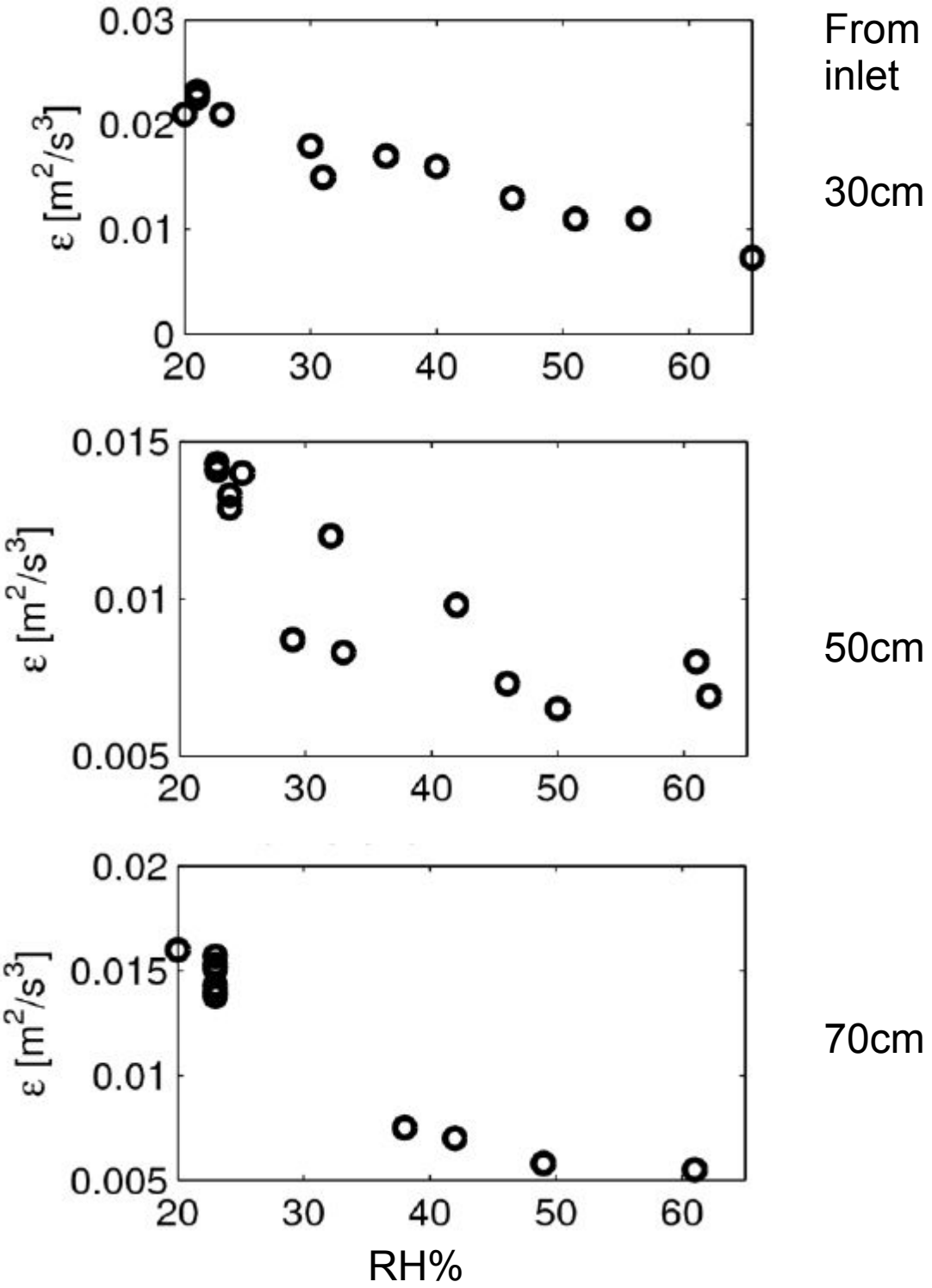

From inlet

30cm

50cm

70cm

Estimates of TKE dissipation rate ε:

- ε increases with decreasing environmental RH;
- far from the source high ε only at low environmental RH.

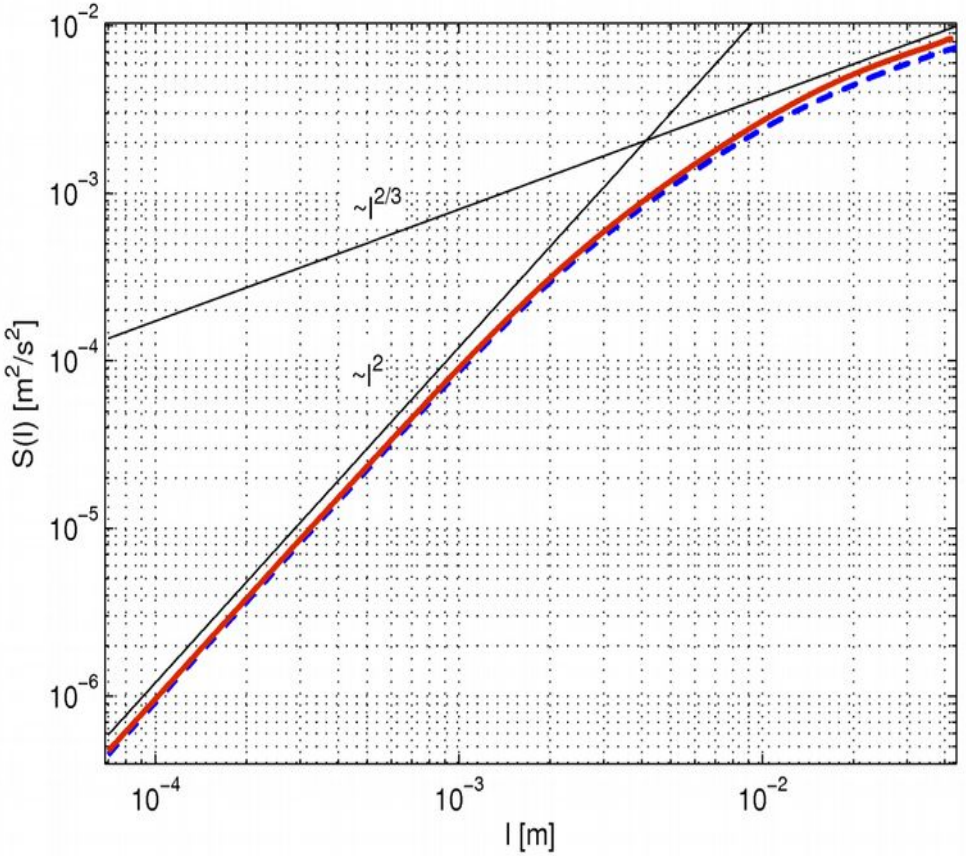

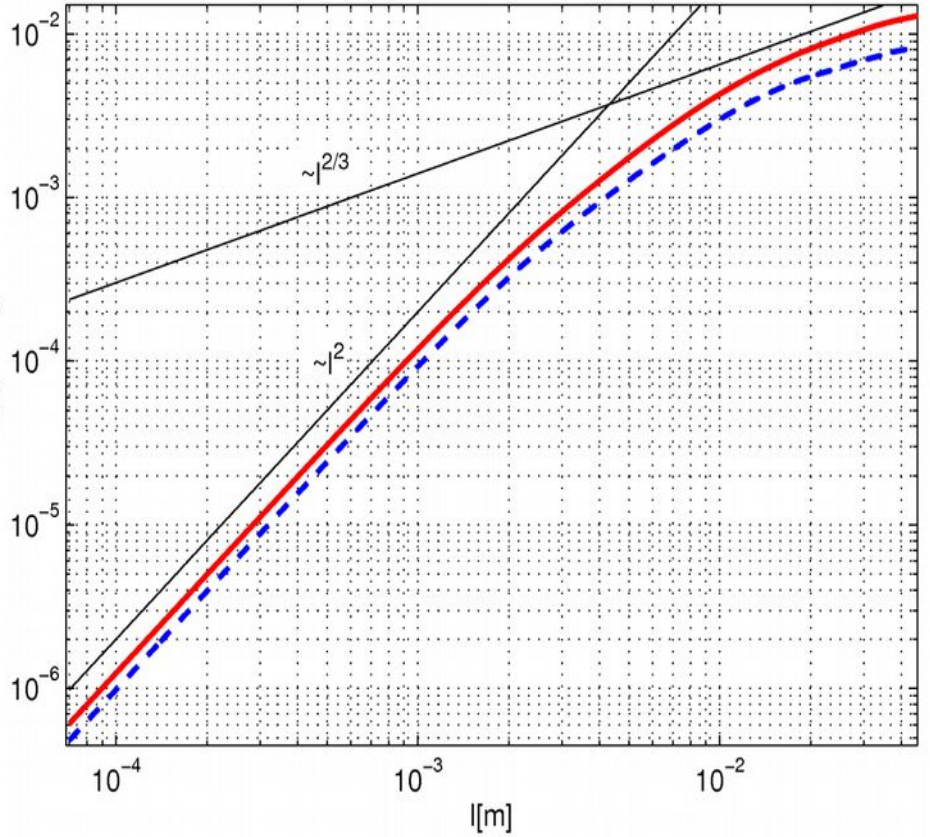

Longitudinal and transversal

structure functions of turbulent velocity fluctuations in the cloud chamber at RH 20% at 70cm from the inlet (red – w' , blue – u')

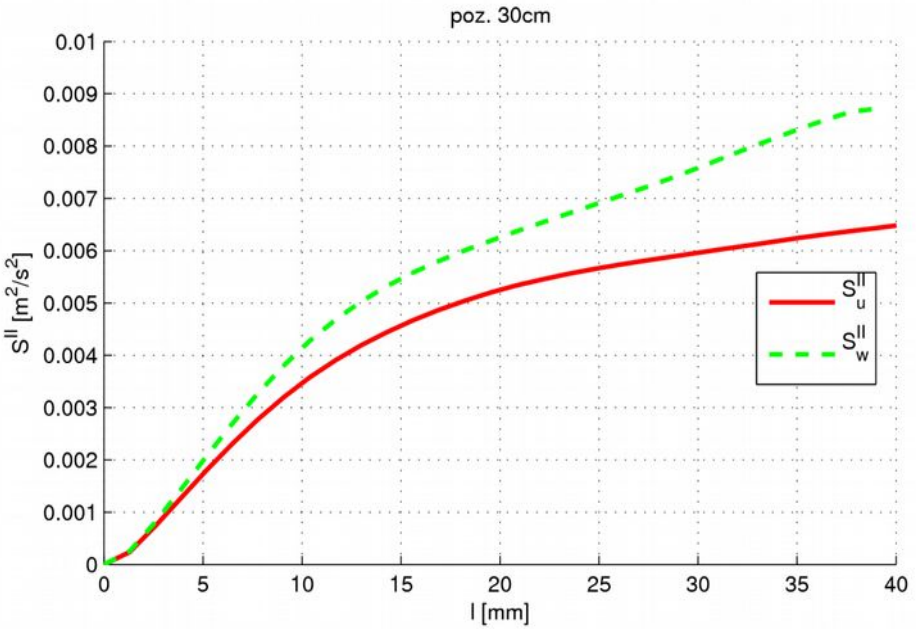

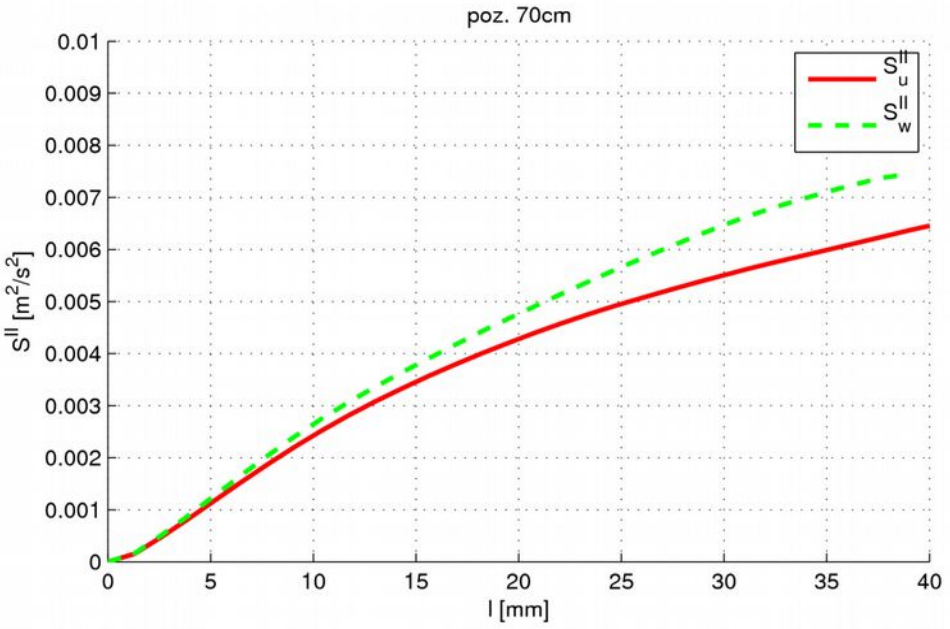

Longitudinal structure functions at RH 20% at 30cm (left) and 70cm (right) from the inlet

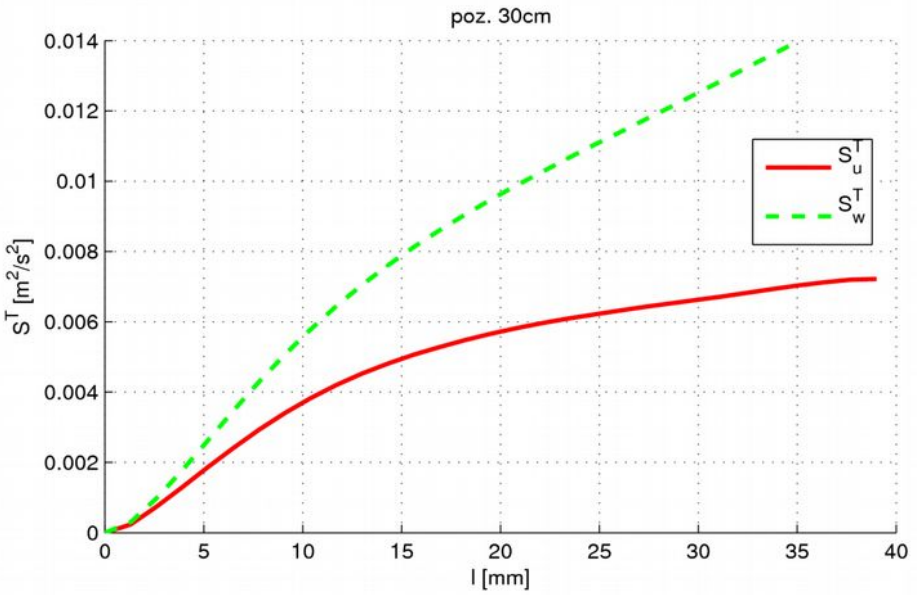

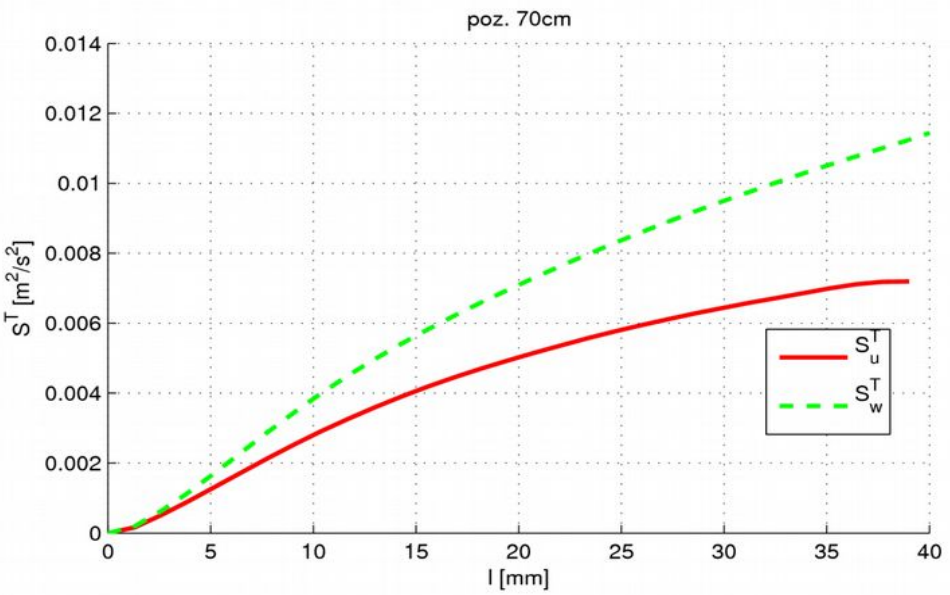

Transversal structure functions at RH 20% at 30cm (left) and 70cm (right) from the inlet

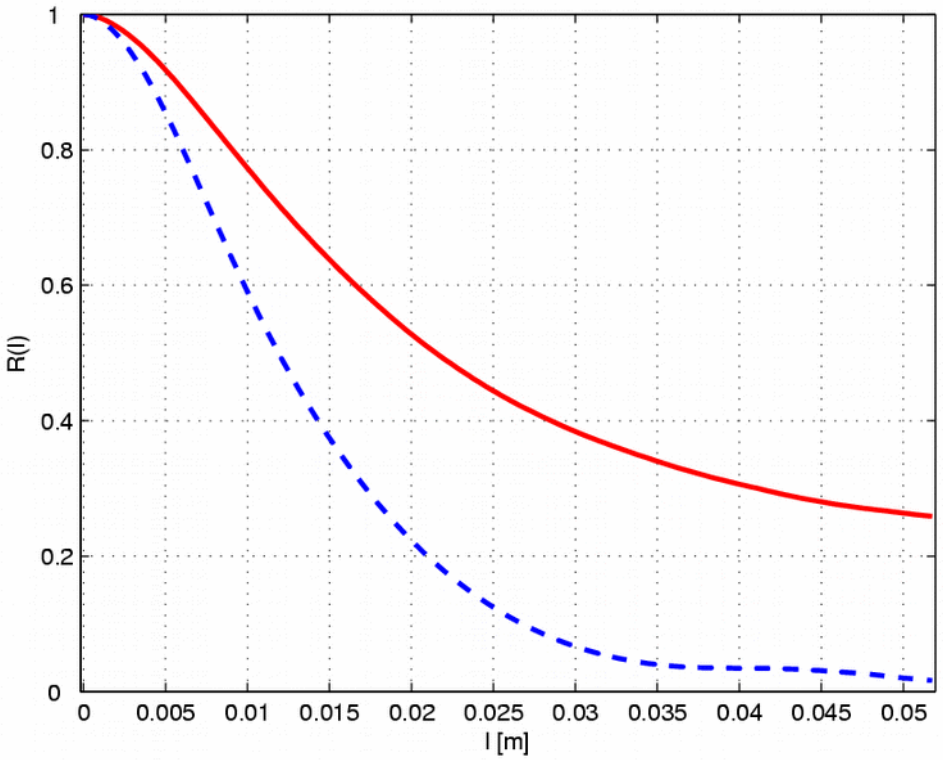

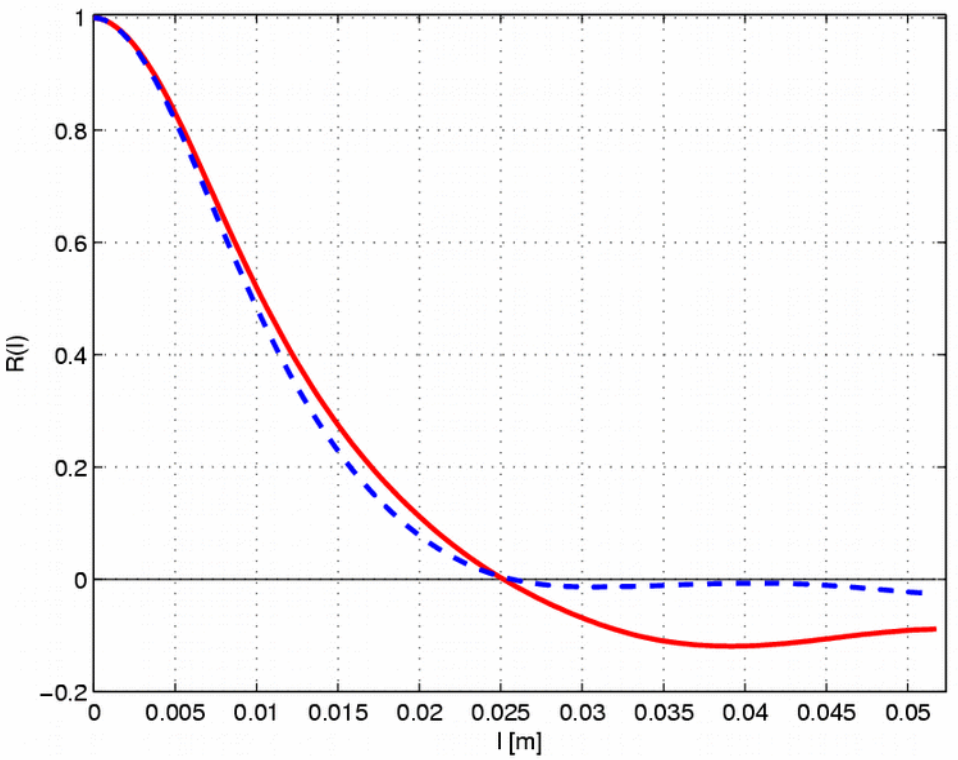

Longitudinal and transversal

autocorelation functions of turbulent velocity fluctuations in the cloud chamber at RH 20% at 70cm from the inlet (red – w' , blue – u')

$\Delta T_{inv} \sim 2°C$

$\Delta h_{inv} \sim 20$ cm

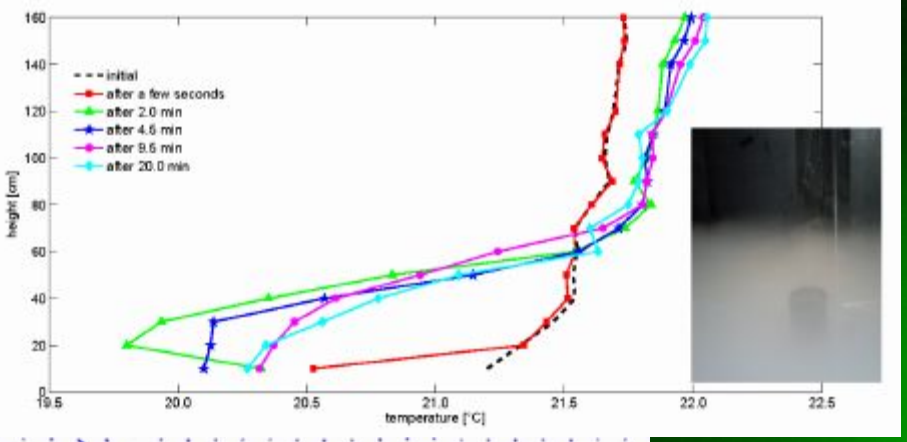

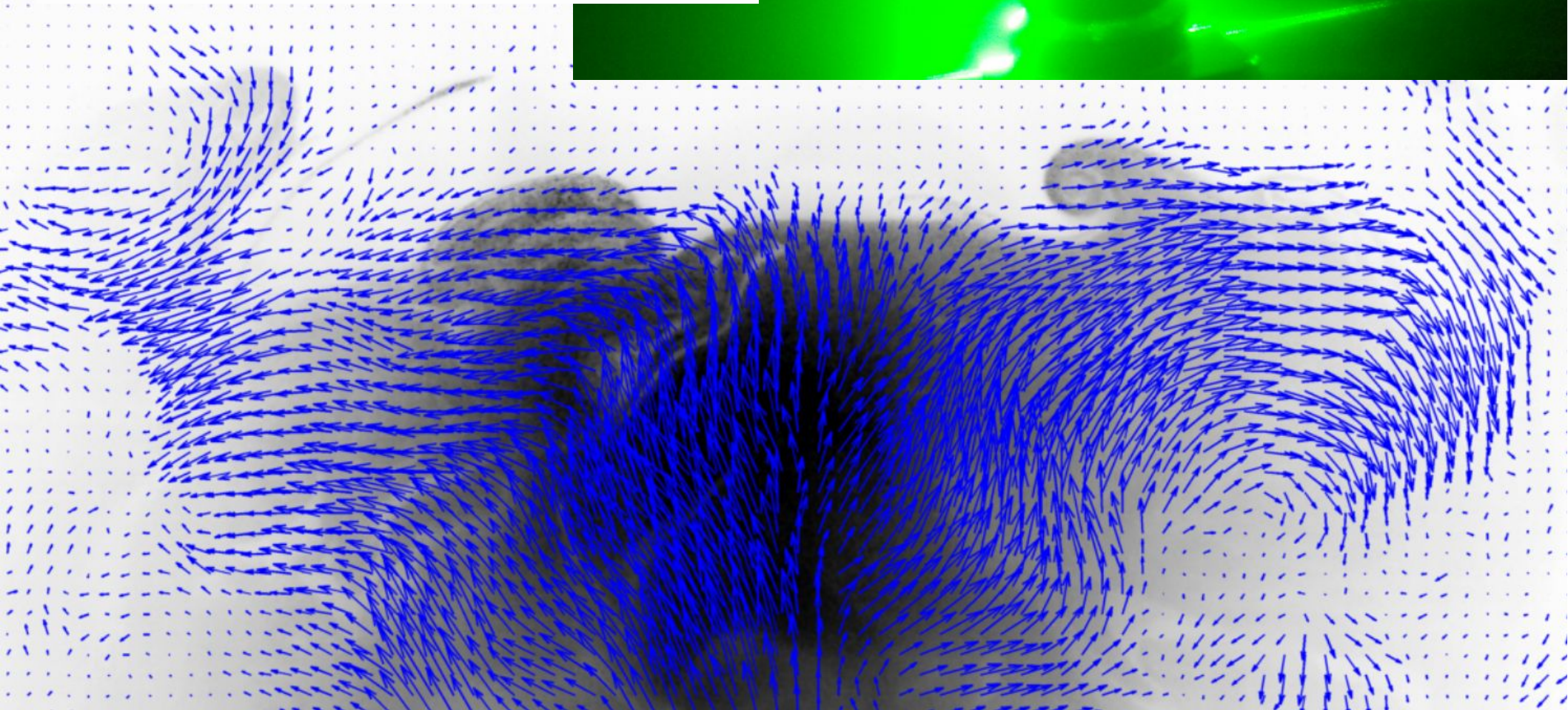

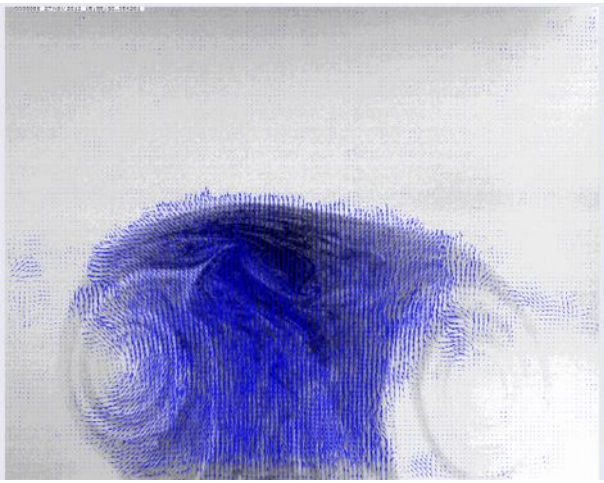
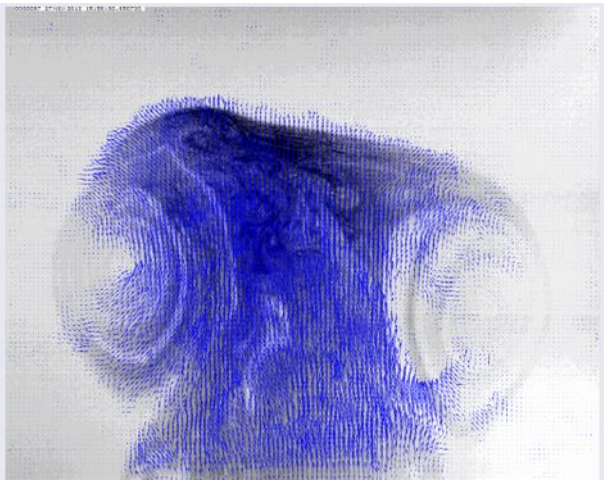
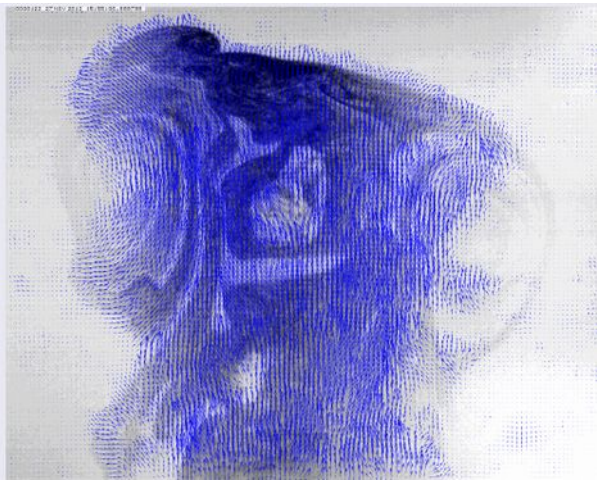
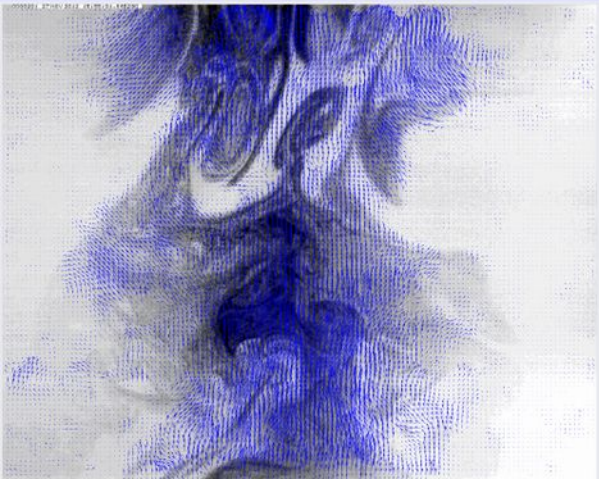
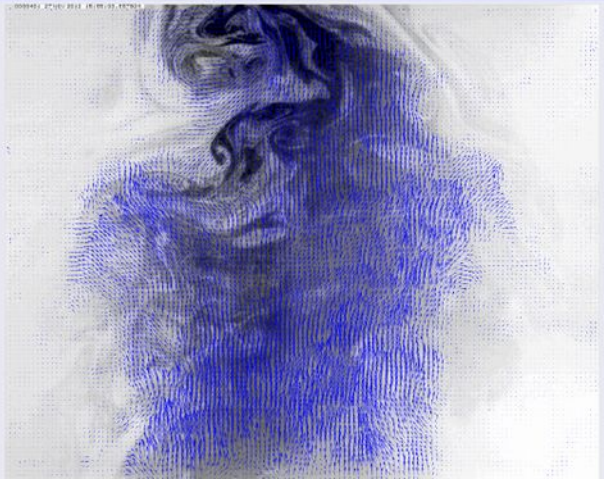
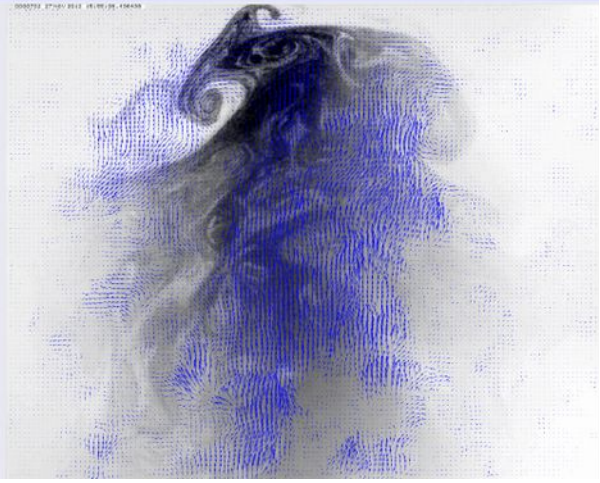

SUMMARY

Mixing of cloud with clear air is a two-phase reacting flow. Influence of submerged heavy particles (cloud droplets) on this flow is important.

In the analyzed scales kinetic energy of microscale motions comes not only from the classical downscale energy cascade, but it is also generated internally due to the evaporation of cloud droplets.

For low TKE mixing and homogenization are dominated by the TKE generated as a result of evaporation of cloud water.

Sedimentation of droplets is important as a transport mechanism of liquid water from cloudy to clear air filaments for low levels of initial TKE.

Enstrophy production by microscale buoyancy fluctuations is substantial, and results in anisotropy of small-scale turbulence.

Temperature measurements in clouds indicate filaments due to cloud-clear air turbulent mixing, supporting the hypothesis that numerical and laboratory studies reflect some aspects of turbulent mixing realized in nature.